NASA TECHNICAL NOTE
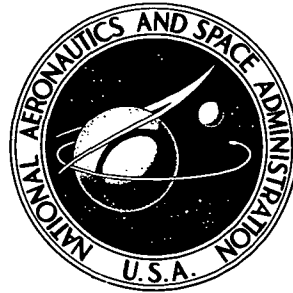
NASA TN D-7075

NASA TN D-7075

NOISE GENERATED BY IMPINGEMENT
OF A JET UPON A LARGE FLAT BOARD

by William A. Olsen, Jeffrey H. Miles,
and Robert G. Dorsch

Lewis Research Center
Cleveland, Ohio 44135

1. Report No. NASA TN D-7075	2. Government Accession No.	3. Recipient's Catalog No.
4. Title and Subtitle NOISE GENERATED BY IMPINGEMENT OF A JET UPON A LARGE FLAT BOARD		5. Report Date December 1972
		6. Performing Organization Code
7. Author(s) William A. Olsen, Jeffrey H. Miles, and Robert G. Dorsch		8. Performing Organization Report No. E-6983
9. Performing Organization Name and Address Lewis Research Center National Aeronautics and Space Administration Cleveland, Ohio 44135		10. Work Unit No. 741-72
		11. Contract or Grant No.
12. Sponsoring Agency Name and Address National Aeronautics and Space Administration Washington, D.C. 20546		13. Type of Report and Period Covered Technical Note
		14. Sponsoring Agency Code

15. Supplementary Notes

16. Abstract

Data were obtained on the noise generated by an air jet impinging on a large flat board. The board was large enough so that the flow leaving the edges of the board generated no significant noise. The impingement angle, nozzle shape and size, jet velocity, and the distance from the nozzle to the board were varied in the experiment. Far-field noise data are presented. The nozzle-alone noise contribution to the total noise was generally small and was subtracted from the total, leaving the impingement-only noise. The impingement-only noise was adequately correlated by eighth power of the peak impingement velocity and first power of the impingement area. The spectral data were correlated by a Strouhal number based on the peak impingement velocity and a characteristic impingement diameter.

17. Key Words (Suggested by Author(s)) Aerodynamic noise Jet impingement Large surfaces	18. Distribution Statement Unclassified - unlimited		
19. Security Classif. (of this report) Unclassified	20. Security Classif. (of this page) Unclassified	21. No. of Pages 35	22. Price* $3.00

CONTENTS

NOISE GENERATED BY IMPINGEMENT OF A JET UPON A LARGE FLAT BOARD

by William A. Olsen, Jeffrey H. Miles, and Robert G. Dorsch

Lewis Research Center

SUMMARY

Data were obtained on the noise generated by an air jet impinging on a large flat board. The board was large enough so that the flow leaving the edges of the board generated no significant noise. The impingement angle, nozzle shape and size, jet velocity, and the distance from the nozzle to the board were varied in the experiment. Far field noise data are presented. The nozzle-alone noise contribution to the total noise was generally small and was subtracted from the total, leaving the impingement-only noise.

The noise generated by an air jet impinging on a very large flat plate has the following major characteristics.

(1) The shape of the total noise (impingement and nozzle) radiation pattern is essentially independent of nozzle velocity and reaches its maximum near 160° from the upstream end of the board.

(2) The impingement-only noise (total sound power level) was correlated by the eighth power of the peak impingement velocity and first power of the impingement area. The spectral data were correlated by a Strouhal number based on the peak impingement velocity and a characteristic impingement diameter. When the jet impingement is not normal, the impingement angle is also brought into the correlation. The total sound power level is proportional to the square of the sine of the impingement angle. The Strouhal number is multiplied by the reciprocal of the square root of the sine of the impingement angle.

INTRODUCTION

In one of the short takeoff and landing aircraft (STOL) concepts, the engine exhaust is deflected downward by a wing with trailing-edge flaps. References 1 to 3 showed that the impingement of the exhaust jet on the flap surfaces results in considerable additional noise. Jet impingement noise also results when an exhaust jet is turned by a thrust reverser or spoiler. In vertical takeoff and landing (VTOL) applications additional noise is generated when the engine exhaust jet is directed at the ground.

As part of the aeronautical research program at the Lewis Research Center, jet impingement noise is being studied. This report contains the results of an investigation wherein a jet was directed at a very simple surface, a large flat board.

Far-field noise data were taken for a jet impinging on the board and for the nozzle alone. The variables of the study were the nozzle exhaust velocity, nozzle diameter and shape, distance from the nozzle to the board and the angle of the board from the nozzle centerline. For most of the data the board was normal to the ground, and the microphones were in a plane parallel to the ground that passed through the nozzle centerline. Limited data were taken to examine the impingement noise for axial symmetry.

APPARATUS AND PROCEDURE

Flow System and Board

Proceeding downstream the flow system (fig. 1) consisted of an orifice for flow measurement, a 10-centimeter globe type of flow control valve, a valve noise quieting
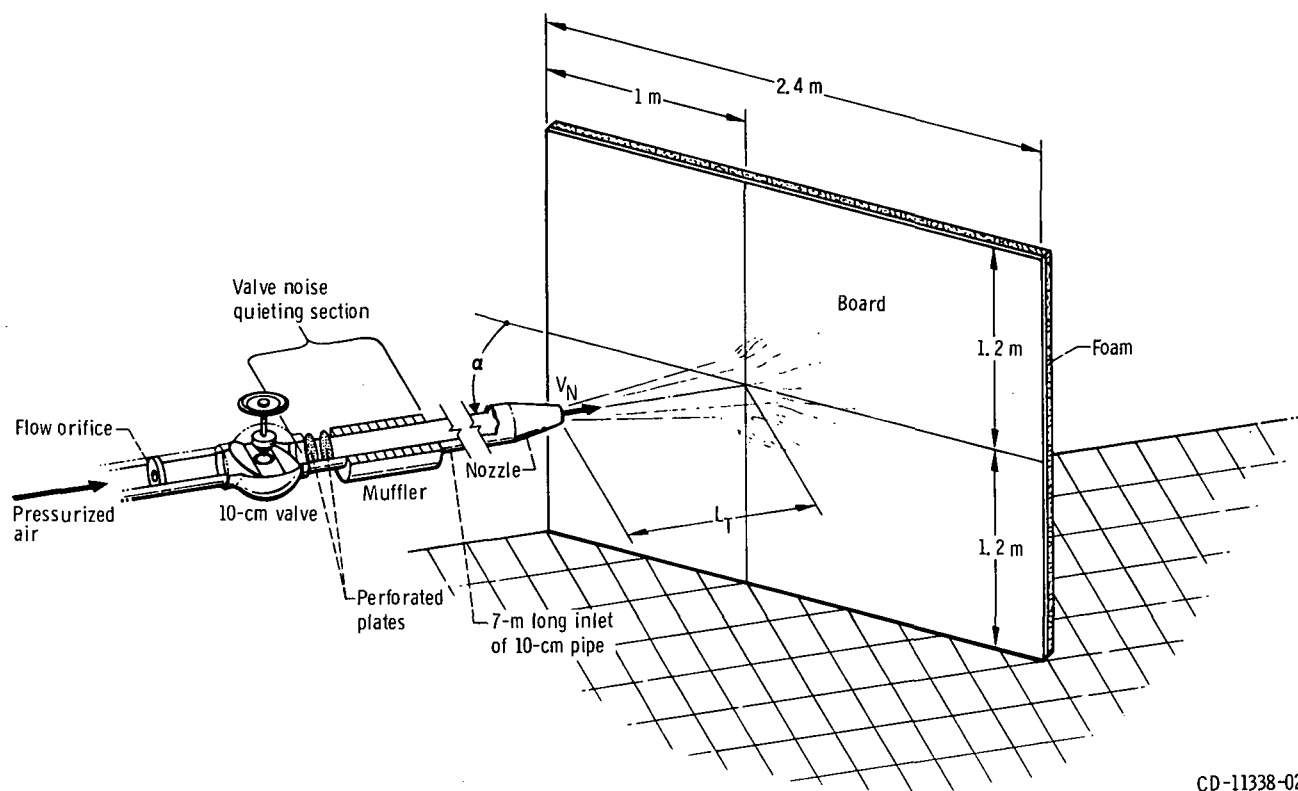
Figure 1. - Flow system and board.

section, a long straight run of 10-centimeter pipe and finally the nozzle. The nominal nozzle stagnation temperature was near ambient. The nozzle jet was directed at near the center of a large flat smooth board (2.4 by 2.4 m). The board rested on the ground and was moved to change the jet impingement distance and angle. It was made of 2.5-centimeter-thick smooth plywood with 10-centimeter-thick foam rubber glued to the back side of the board.

Valve noise was not a problem in this experiment for the following reasons. The flow system and quieting section are the same as those used in reference 2. In that study it was shown that for nozzle exhaust velocities V_N greater than 190 meters per second, the noise generated by the nozzle alone followed a V_N^8 relation. (Symbols are defined in the appendix.) The spectral distribution followed that reported in reference 4. In addition, the noise levels of the board noise are generally much greater than the nozzle-alone noise levels.

Acoustic Instrumentation

The noise data were measured by 1.3-centimeter (half inch) condensor microphones with windscreens. The microphones were located in a horizontal plane that passed through the nozzle centerline. The microphones were placed on a 3-meter-radius circle (see fig. 2) that enclosed the board and nozzle. Eight microphones (on one side of the centerline) were used when the board was normal to the nozzle centerline ($\alpha = 90^O$) or when the nozzle-alone noise data were taken. Fourteen microphones were placed around the entire microphone circle when the board was not normal to the centerline ($\alpha < 90^O$). The angle α is the minimum angle from the board to the nozzle centerline. In both cases the microphones were more concentrated on the microphone circle wherever the noise level was highest. The microphones were kept out of any high velocity exhaust jet.

Most of the noise data were taken with the board normal to the ground and microphone circle ($\varphi_B = 0^O$) because this is the orientation of maximum noise. The noise is axisymmetric for the board at $\alpha = 90^O$ and for the nozzle alone. The noise in the minimum noise plane ($\varphi_B = 90^O$) for the nonaxisymmetric case of $\alpha = 60^O$ was also measured. This was accomplished by rotating the board counterclockwise 90° about the nozzle centerline, while holding $\alpha = 60^O$ (fig. 2). This means that the board is at an angle of 60° to the ground. This $\varphi_B = 90^O$ case is geometrically equivalent to leaving the board normal to the ground at $\alpha = 60^O$, as in the $\varphi_B = 0^O$ case, and then rotating the microphone plane 90° (clockwise) about the nozzle centerline.
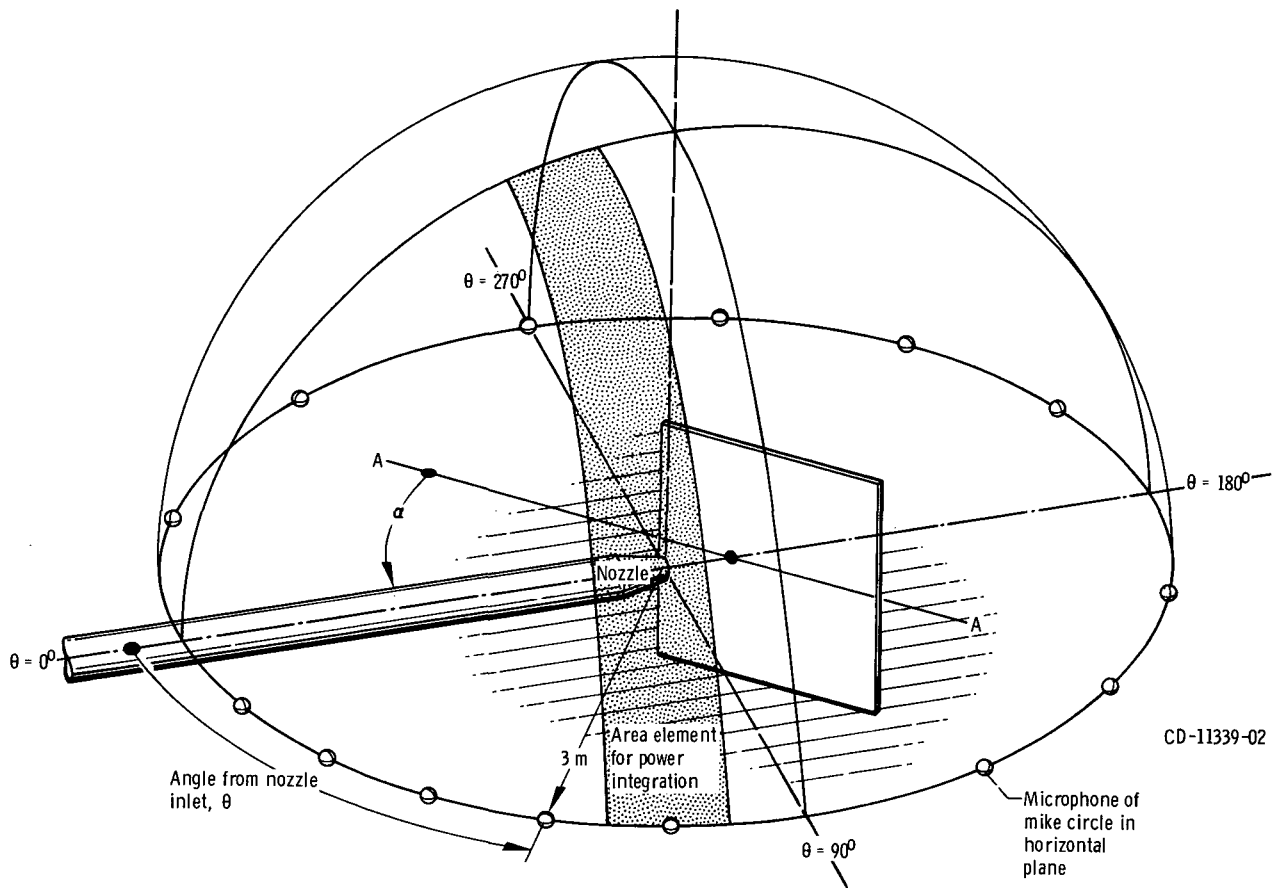
3

Figure 2. - Microphone setup and area element used in the noise power integrations. Board is shown perpendicular to the microphone plane, $\varphi_\theta = 0^o$.

Test Procedure

Far field noise and flow data were taken for as many as five nozzle exhaust velocities ranging from about V_N = 140 to 350 meters per second for the board and nozzle alone. In addition, the distance from the nozzle to the board L_T and impingement angle α were varied. These geometric parameters were set up with respect to the nozzle lip by using a set of templates. The circular nozzle diameter d_N and nozzle shape were also varied. The variables for each test run are listed in table I.

Three noise data samples were taken at each microphone location for each run condition. These data were analyzed directly by a one-third octave band spectrum analyzer. The analyzer calculated sound-pressure-level spectra in decibels referenced to 2×10^{-5} newtons per square meter (0.0002 μbar). The three samples were then arithmetically averaged, and a correction was applied for any microphone, cable, and atmospheric losses. No spectral corrections were deemed necessary for ground reflections because,

4

TABLE I. - EXPERIMENTAL CONVERGENT NOZZLE AND ORIFICE PLATE PARAMETERS

Run day-run number	Nozzle description					Nozzle exhaust velocity, V_N, m/sec	Impingement length to nozzle diameter ratio, L_T/d_N	Impingement angle, α, deg	Azimuthal angle, φ_B, deg	Conditions, $(A)_{a,b}$ = Vary A holding a and b constant	Typical nozzle stagnation temperature,[a] T_N, K	Peak impingement velocity, V_{ip}, m/sec	Characteristic impingement diameter, d_i, m
	Type	Nozzle diameter, d_N, cm	Orifice plate description										
			Orifice shape	Hole diameter, cm	Hole spacing, cm								
7-80	Convergent[b]	5.2	---------	----	---	292	Nozzle alone, no board	Nozzle alone, no board	Nozzle alone, no board	-----------------	284	---	------
7-81			---------	----	---	195				-----------------		---	------
[c]7-82			---------	----	---	130				-----------------		---	------
7-83			---------	----	---	344				-----------------		---	------
6-50			---------	----	---	236				-----------------		---	------
13-04		4.1	---------	----	---	289				-----------------	290	---	------
13-05		4.1	---------	----	---	193				-----------------		---	------
13-06		2.7	---------	----	---	191				-----------------		---	------
13-07		2.7	---------	----	---	288				-----------------		---	------
6-52		7.8	---------	----	---	196				-----------------	284	---	------
14-45	Orifice plates	---	Four holes	4.1	6.4	290	Nozzle alone, no board	Nozzle alone, no board	Nozzle alone, no board	-----------------	300	---	------
14-46	of same	---	Four holes	----	1.9	296				-----------------		---	------
14-54	hole area	---	16 holes	1.03	1.0	295				-----------------		---	------
14-49		---	Vertical slot 1.04×12.7 cm	----	---	287				-----------------		---	------
9-06	Convergent	5.2	---------	----	---	188	7.05	60	0	$(V_N)_{L_T}, \alpha, d_N$	278	168	0.0374
9-07			---------	----	---	286	7.05	60			278	256	.0374
5-61			---------	----	---	338	7.05	60			274	322	.0426
12-88			---------	----	---	340	9.7	90			290	290	.0426
12-89			---------	----	---	289						206	.044
12-90			---------	----	---	193						137	
12-91			---------	----	---	236						181	
12-92			---------	----	---	289						206	
12-93			---------	----	---	141						103	
16-93			---------	----	---	240	7.05				300	221	.0374
16-94			---------	----	---	192						171	.0374
[d]16-95			---------	----	---	295						264	.0374
16-96			---------	----	---	350						334	.0426
16-97			---------	----	---	138						125	.0412

TABLE I. - Concluded. EXPERIMENTAL CONVERGENT NOZZLE AND ORIFICE PLATE PARAMETERS

Run day-run number	Nozzle description					Nozzle exhaust velocity, V_N, m/sec	Impingement length to nozzle diameter ratio, L_T/d_N	Impingement angle, α, deg	Azimuthal angle, φ_B, deg	Conditions, $(A)_{a,b}$ = Vary A holding a and b constant	Typical nozzle stagnation temperature,[a] T_N, K	Peak impingement velocity, V_{ip}, m/sec	Characteristic impingement diameter, d_i, m
	Type	Nozzle diameter, d_N, cm	Orifice plate description										
			Orifice shape	Hole diameter, cm	Hole spacing, cm								
9-7	Convergent	5.2	---------	----	---	286	7.05	60	0	$(\alpha)V_N, L_T, d_N$	278	256	0.0374
9-8			---------	----	---			30					
9-9			---------	----	---			15					
9-10			---------	----	---			90					
12-94			---------	----	---	293	1.88			$(L_T)\alpha, V_N, d_N$		290	.052
[e]12-95			---------	----	---		4.7					290	.042
12-96			---------	----	---		14.5					155	.044
12-97			---------	----	---		25					88	.07
12-89, -92			---------	----	---	289	9.7					206	.044
[d]12-87			---------	----	---	289	7.05					267	.0374
14-51			---------	----	---	297	2.8				300	294	.046
14-52			---------	----	---	297	1.43				300	294	.052
16-95			---------	----	---	295	7.05				300	264	.0374
12-89			---------	----	---	289	9.7			$(d_N)\alpha, V_N, L_T/d_N$	278	206	.044
12-98		2.7	---------	----	---	289	9.7				278	206	.022
13-02		4.1	---------	----	---	289	9.7				290	206	.034
9-6		5.2	---------	----	---	188	7.05	60			289	167	.0374
11-36		2.7	---------	----	---	186					275	166	.019
9-12		4.1	---------	----	---	188					278	167	.0296
16-90		7.8	---------	----	---	190					300	170	.0556
9-7		5.2	---------	----	---	286					289	256	.0374
9-13		4.1	---------	----	---	283					278	253	.0296
9-11		2.7	---------	----	---	281					278	251	.019
14-42	Orifice plates	---	Four holes	4.1	6.4	290	7.35	90	0	Nozzle shape at constant V_N, L_T, and nozzle area	.300	[f]230	0.016
14-32	of same	---	Four holes	4.1	6.4	290	24.5					[g]127	.056
14-47	hole area	---	Four holes	----	1.9	296	7.35					[f]246	.016
14-53		---	16 holes	1.03	1.0	295	14.7					[g]160	.052
14-50		---	Vertical slot 1.04×12.7 cm		---	287	14.5					[i]173	.042
(e), (j)		---	One hole	4.13	---	295	3.7					[h]280	.0296
16-88	Convergent	5.2	---------	----	---	293	7.05	60	0	$(\varphi_B)V_N, L_T/d_N$	300	262	0.0374
16-91			---------	----	---	293			90			262	
16-89			---------	----	---	192			0			171	
16-92			---------	----	---	192			90			171	

[a]Ambient air temperature is typically 2 K lower than stagnation temperature.
[b]The nozzle has a 0.32-cm lip.
[c]Valve noise present.
[d]Whistle.
[e]Screech.
[f]Four circular jets.
[g]One well mixed circular jet.
[h]One circular jet.
[i]One rectangular jet.
[j]No noise data taken.

generally, the major cancellations and reinforcements occur at much lower frequencies than the region of interest. The overall sound pressure level OASPL at each microphone position θ was computed from the averaged and corrected sound-pressure-level spectrum SPL. The sound-power-level spectrum PWL and total sound power level PWL$_t$ were computed by spatial integration of the SPL data from each microphone. The values of SPL and OASPL at each microphone position already include the ground reflection contribution. Therefore, the spatial integrations for sound power is made over a hemisphere. Because most of the noise data are axisymmetric (e. g., nozzle-alone and board at $\alpha = 90^o$) the integration was performed using the "half-bread-slice" area elements shown in figure 2. When the noise was axisymmetric the correct, PWL would be computed. But when $\alpha < 90^o$ the noise is not axisymmetric and only an approximate measure of the sound power level is computed PWL'. This is evaluated from data taken in the φ_B plane by assuming that there is no azimuthal variation (with φ_B) of the noise.

The condensor microphones were calibrated before each day of running with a standard piston calibrator (a 124-dB, 250-Hz tone). The one-third octave band analyzer was calibrated before each test with a constant voltage source and checked during the experiment with an electronic pink noise generator. The data acquisition and data analysis systems were further checked by the experimentor by repeated runs and by a uniform directivity orifice noise source of a 1.5-decibel repeatability. Considering these calibrations and checks, repeated data, and the averaging of three widely spaced (in time) samples of data, it is estimated that the reported data are repeatable to within 1.5 decibels from day to day. Most of the directly compared data were obtained on the same day so that those data are repeatable to about 1/2 decibel.

RESULTS AND DISCUSSION

Placing a large flat board in the high velocity jet of a nozzle affects the noise measured in essentially four ways:

(1) The impingement of the jet on the board surface generates additional noise to the nozzle-alone noise. But no additional noise is generated by the air leaving the edge of the board because its velocity is too low (measurements showed that it was an order of magnitude lower than the impingement velocity).

(2) The board redirects (by reflection and shielding) the noise generated by the nozzle alone and any internal noise (e. g., valve noise).

(3) Less low-frequency nozzle-alone jet noise is generated as the board is brought closer to the nozzle.

(4) A feedback noise (narrowband whistle or screech) can occur for certain flow and configuration conditions (ref. 5).

The primary purpose of this report is to determine the effect of the experimental parameters (nozzle exhaust velocity, impingement angle and distance, and nozzle shape) on the additional aerodynamic noise generated by impingement of the jet on a large flat board. The best way to accomplish this is to work with the sound power level spectrum because, ideally, it is not affected by the redirection of noise. These spectra are then corrected to exclude the noise from the nozzle alone (i. e., PWL generated by the nozzle without the board), and also to exclude any additional narrowband noise caused by feedback whistle or screech. Unfortunately, a power spectrum requires sound measurements in all azimuthal planes if $\alpha < 90^O$. Most of the board noise data in this report were taken for cases where there was normal jet impingement, $\alpha = 90^O$. For these cases and for the nozzle-alone cases the noise is axisymmetric and measurements need to be taken in only one azimuthal plane ($\varphi_B = 0^O$).

Complete tables of the one-third octave SPL and PWL spectra are available from the authors on request.

Noise Radiation Patterns

In this section some representative noise radiation patterns are shown to acquaint the reader with the data before the power spectra are discussed. These plots show the effect of nozzle exhaust velocity and impingement angle on the noise patterns that result when the jet from a nozzle is directed at a very large flat board. Most of the noise patterns are in the plane of maximum noise ($\varphi_B = 0^O$). Some data were also taken in the minimum noise plane ($\varphi_B = 90^O$).

Figure 3 shows the variation of OASPL with θ for the board normal to the ground ($\varphi_B = 0^O$) for various velocities at $L_T = 37$ centimeters and $d_N = 5.2$ centimeters. Figure 3(a) shows the data for $\alpha = 90^O$ (normal impingement) and figure 3(b) shows the data for $\alpha = 60^O$. In both cases the noise radiation patterns are similar in shape over the range of velocity shown. The noise level for normal impingement (fig. 3(a)) is essentially independent of θ on the nozzle side of the board and falls off rapidly behind it.

Figure 4 contains a plot of the noise radiation patterns that result, in the $\varphi_B = 0^O$ plane at $L_T = 37$ centimeters and $V_N = 286$ meters per second, when the jet impingement angle α is varied. These patterns are plotted with respect to the board ($\theta + \alpha$) rather than with respect to the nozzle inlet θ. This figure shows that as α increases the noise level increases, especially for ($\theta + \alpha$) less than 140°. But the maximum OASPL, which occurs at about ($\theta + \alpha$) = 160°, does not change much. The OASPL plotted here is the sum of the impingement and nozzle-alone noise. The nozzle-alone
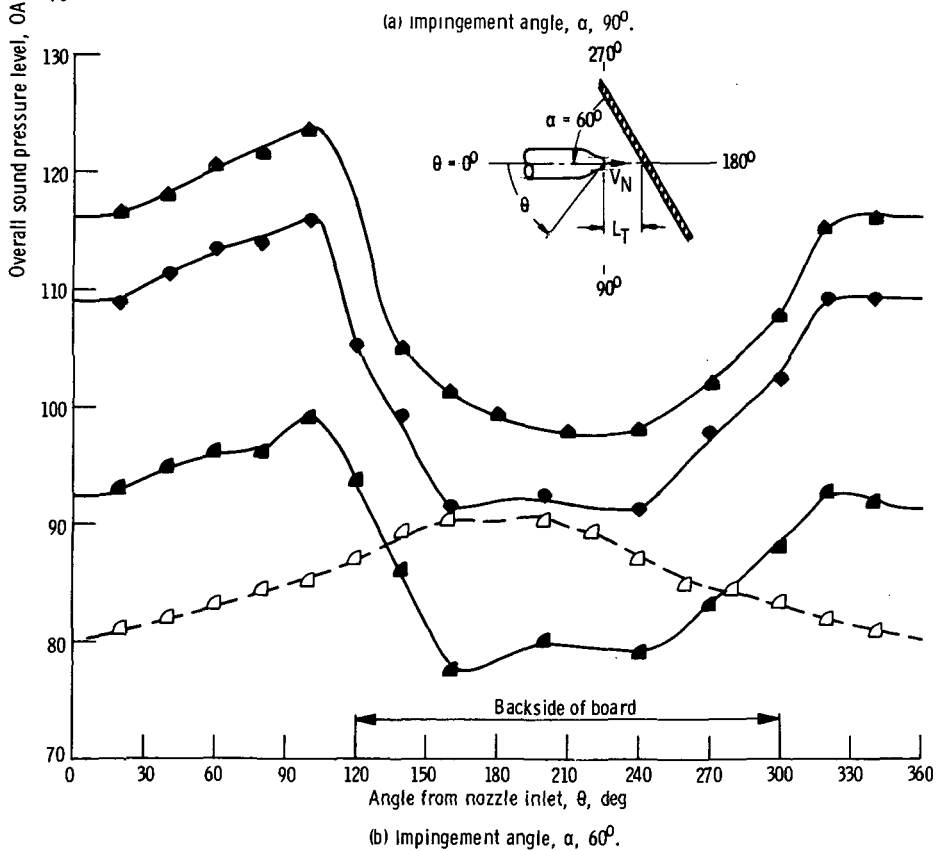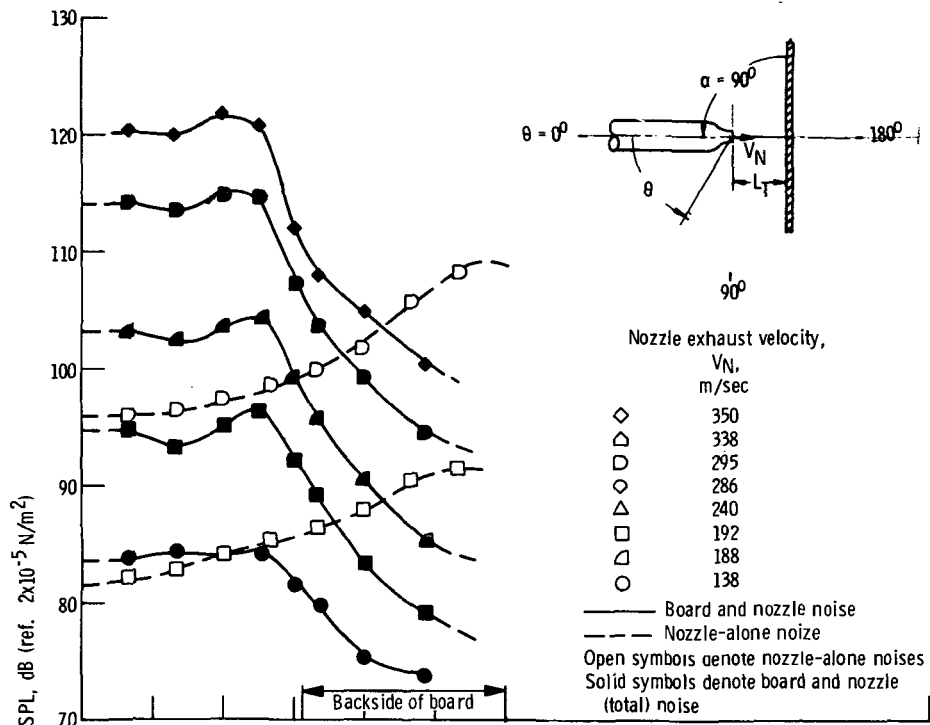
Figure 3. – Noise radiation patterns for jet impinging on board at several nozzle exhaust velocities. Azimuthal angle, φ_B, 0°; nozzle diameter, d_n, 5.2 centimeters; impingement distance, L_T, 37 centimeters.
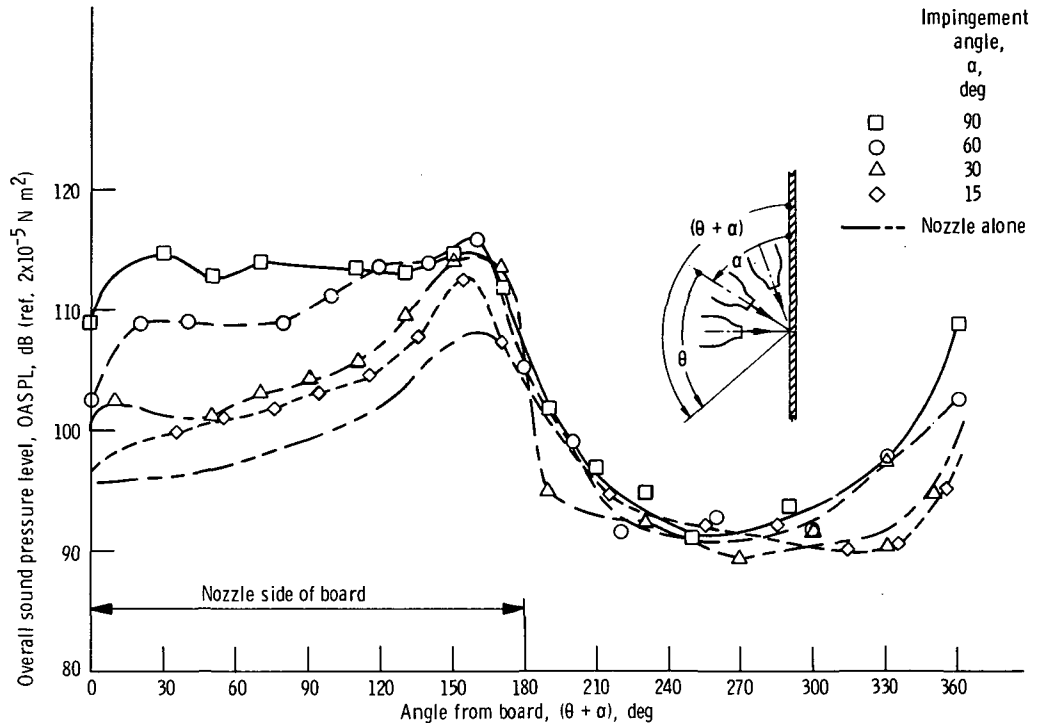
9

Figure 4. – Effect of impingement angle, α, on noise radiation pattern of board. Azimuthal angle, φ_B, 0°; nozzle exhuast velocity, V_N, 286 meters per second; impingement distance, L_T, 37 centimeters; nozzle diameter, d_N, 5. 2 centimeters.

noise pattern is also plotted in this figure, with α taken as 0°. Figure 4 shows that the nozzle-alone noise pattern is approached as the impingement angle α approaches 0°. The nozzle-alone noise has its maximum near $\theta = 160^O$, and this noise is of high frequency, which reflects off the large board somewhat like light rays. Therefore, it is understandable that the total noise of the board and nozzle would tend to peak at $(\theta + \alpha) = 160^O$ also.

Limited data were taken to show the azimuthal variation (with φ_B) of the noise radiation pattern. Noise data were taken in the maximum noise orientation ($\varphi_B = 0^O$) where the board was at $\alpha = 60^O$. Then the board at $\alpha = 60^O$ was rotated 90° counterclockwise about the nozzle centerline to $\varphi_B = 90^O$, and the data were taken for this minimum noise orientation. The difference in OASPL between the maximum noise orientation and minimum noise orientation is plotted on figure 5 as a function of θ for two nozzle exhaust velocities. The curves drawn through both sets of data show that, except near $\theta = 90^O$, the azimuthal variation is insensitive to the nozzle exhaust velocity. An average curve drawn through the data has skew symmetry about the indicated point of symmetry. The location of this point imply, that on the average the maximum noise orientation ($\varphi_B = 0^O$) is noisier than the minimum noise orientation ($\varphi_B = 90^O$).
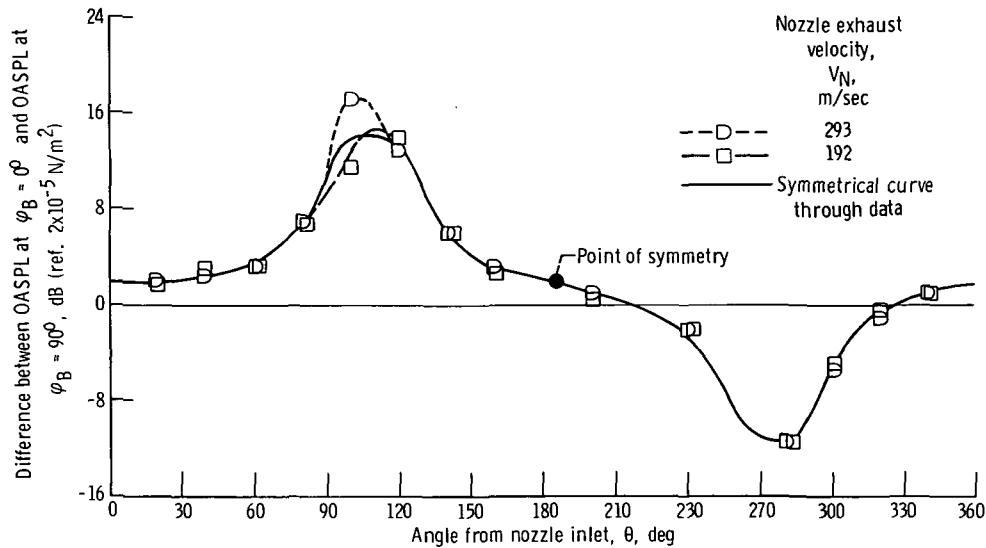
10

Figure 5. - Change in overall sound pressure level from maximum noise plane (φ_B = 0°) to minimum noise plane (φ_B = 90°). Impingement angle, α, 60°; impingement distance, L_T, 37 centimeters; nozzle diameter, d_n, 5.2 centimeters.

Effect of Nozzle Exhaust Velocity on Power Spectra

Data that show the effect of nozzle exhaust velocity on noise will be analyzed in detail in this section. The power spectra will be corrected for nozzle-alone noise, and one data point will be corrected for feedback whistle. From reference 6 it may be expected that the noise generated by the impingement of a jet on a surface would be related to the impingement velocity. The relationship with noise can also be with the nozzle exhaust velocity V_N because V_N is proportional to the impingement velocity for the same nozzle diameter, impingement angle, and distance (ref. 7). The nozzle-alone noise (i.e., PWL generated by the nozzle without the board) for a 5.2-centimeter nozzle is plotted in figure 6 for several values of V_N. Figure 7 contains the PWL for the total noise generated by the nozzle and by the impingement of the jet on the board at $\alpha = 90^o$ and L_T = 37 centimeters.

Before the nozzle noise is subtracted from the total noise to obtain the impingement-only noise, there are some items to discuss about the results plotted in figures 6 and 7.

The significant ground-reflection cancellations and reinforcements occur within the one-third octave filters denoted, respectively, for C_i and R_i in figures 6 and 7. The largest effect is at the lowest velocity. No spectral correction was made to smooth out these spectra because the effect on the results was found to be generally insufficient to warrant the effort of correcting the spectra. The spatial integration to obtain the PWL spectra was made over a hemisphere. This accounts for the fact that at high frequency,
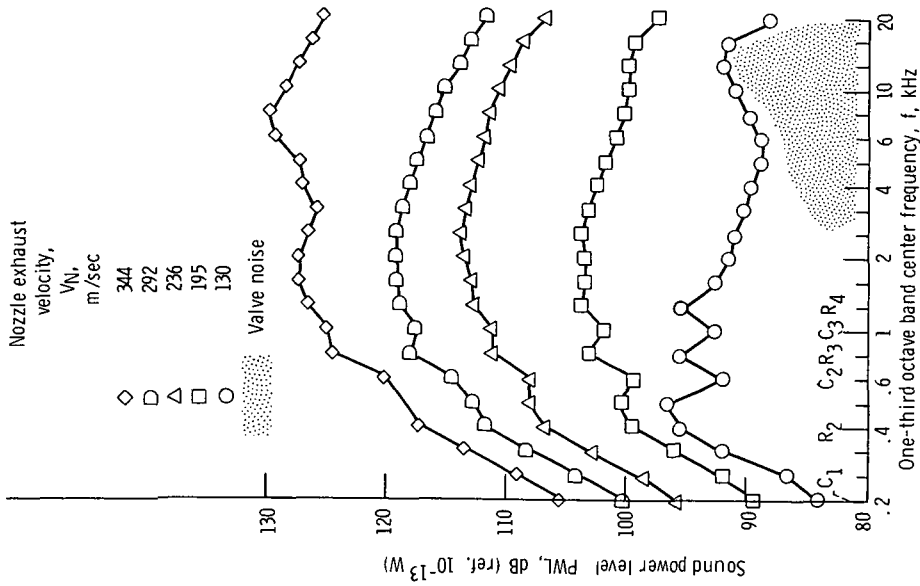
11
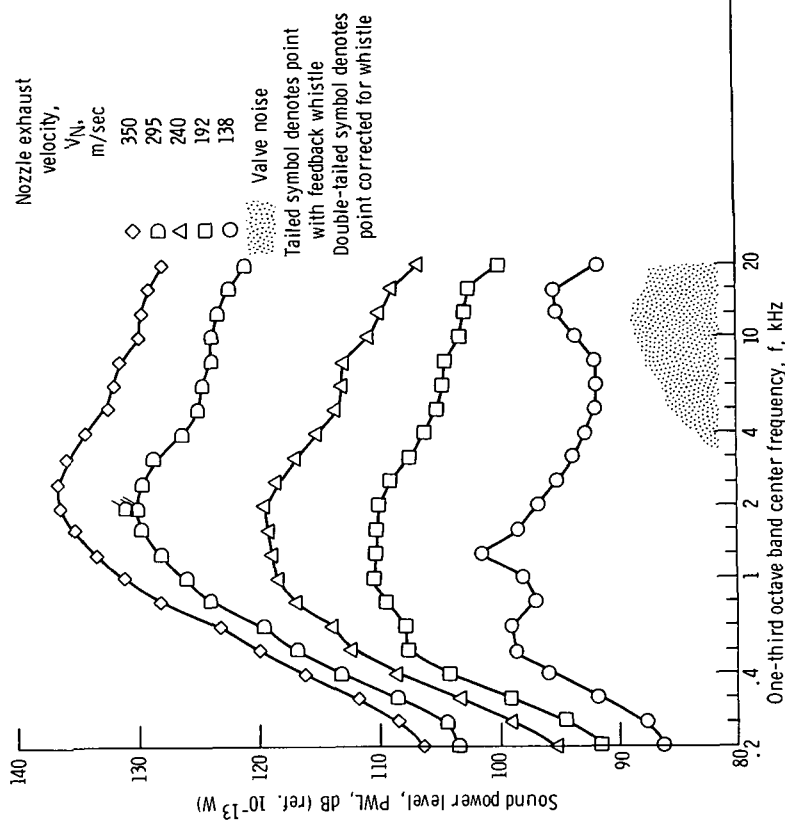
Figure 7. – Sound power level spectra generated by jet impinging on board at several nozzle exhaust velocities. Impingement angle, α, 90^0 (axisymmetric noise measured at $\varphi_B = 0^0$); impingement distance, l_T, 37 centimeters; nozzle diameter, d_N, 5.2 centimeters.

Figure 6. – Sound power level spectra for nozzle-alone at several nozzle exhaust velocities. Nozzle diameter, d_N, 5.2 centimeters. Ground reflection cancellation and reinforcement frequencies are denoted by C_i and R_i, respectively.

12

where most of the significant data occurs, the microphone output includes the ground-reflection contribution. Because the impingement of the jet is normal ($\alpha = 90^\circ$) for figures 6 and 7, the sound field is axisymmetric. The nozzle-alone noise is also axisymmetric; therefore, the spatial integration performed, which assumed axial symmetry, results in a true PWL spectrum for these cases.

The high-frequency bump in the nozzle-alone spectrum in figure 6 at $V_N = 344$ meters per second is due to broadband shock noise (ref. 8). This nozzle-alone shock noise does not show up strongly in the total noise in figure 7 because the impingement-only noise greatly exceeds the nozzle-only noise. The high-frequency bump at the lowest velocity in figures 6 and 7 is due to unattenuated high-frequency valve noise (shaded area). These are the only data showing any significant valve noise, and its affect on the lower frequency impingement only noise is negligible.

The board at $L_T = 37$ centimeters is about 7 nozzle diameters from the nozzle exit. Therefore, only the very low-frequency part of the nozzle-alone noise spectrum could be cut off by the presence of the board. This effect is therefore not important. It is discussed further in the section Effect of Impingement Distance.

A slight feedback noise (whistle) occurred at 2 kilohertz for the case of the board at $V_N = 295$ meters per second. Since feedback noise is essentially an add-on narrowband noise, it is easily corrected when it makes only a small increase in the one-third octave frequency band. The data point with this whistle is plotted in figure 7 as a tailed symbol, which is corrected (-1 dB), based on narrowband data, to the double-tailed symbol.

The sound power spectra (in watts) for the nozzle-alone is now subtracted from the screech corrected sound power spectra for the total noise (board + nozzle). This difference defines the impingement-only noise PWL_C. The nozzle-alone noise data were corrected for small discrepancies with the nozzle exhaust velocities of the board data, by scaling the nozzle-alone noise by V_N^8. Only the lowest velocity case in figures 6 and 7 required a significant correction (2 dB). Figure 8 contains the resulting corrected sound power level spectra PWL_C for the impingement-only noise. Whenever the difference in PWL (e.g., difference in PWL in figs. 6 and 7) is greater than 4 decibels, an open symbol is used. If the difference is between 2 and 4 decibels, a solid symbol is used. A 4-decibel difference would mean that the nozzle-alone noise adds about 2 decibels to the total noise. For most of the peak noise data this difference is greater than 7 decibels (i.e., the nozzle adds less than 1 dB to the total). If the difference is less than 2 decibels, the curve is estimated (dashed line) such that its shape is similar to the other curves in the figure. (This symbolism will be used for all the data that follow.) Similar data were taken over a range of V_N for $\alpha = 90^\circ$ and $L_T = 51$ centimeters. These were similarly corrected and the resulting values of PWL_C are plotted in figure 9.
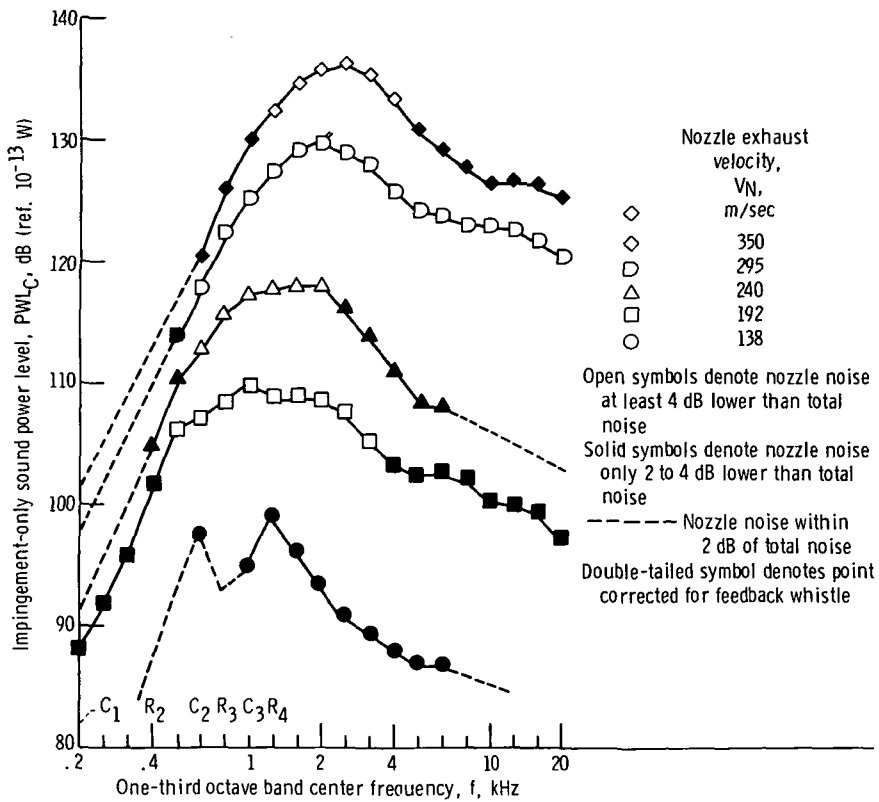
Figure 8. - Impingement-only sound power level spectra for the board. Impingement angle, a, 90°; impingement distance, L_T, 37 centimeters; nozzle diameter, d_N, 5.2 centimeters.
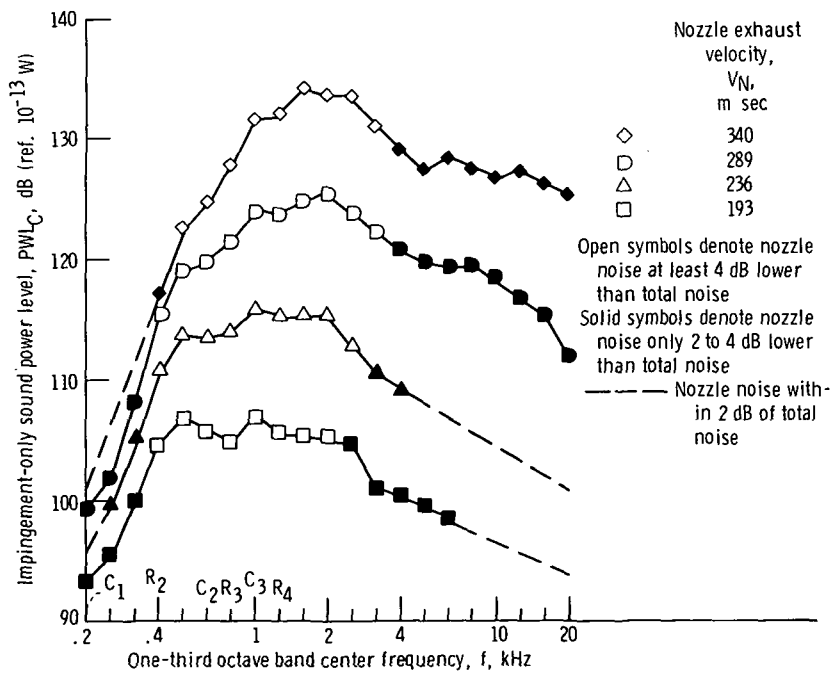

Figure 9. - Impingement-only sound power level spectra at impingement distance, L_T, of 51 centimeters. Impingement angle, a, 90°; nozzle diameter, d_N, 5.2 centimeters.

These corrected spectra for the impingement only noise are then summed up to obtain the impingement only total sound power level PWL_{CT}. Figure 10 contains a plot of PWL_{CT} as a function of V_N for the data in figures 8 and 9, where $\alpha = 90^{\circ}$ and $L_T = 37$ and 51 centimeters. Figure 10 also contains a plot of PWL'_{CT} (evaluated at $\varphi_B = 0^{\circ}$) results for $\alpha = 60^{\circ}$ and $L_T = 37$ centimeters. An eighth power curve V_N^8 fits through each individual set of data in figure 10 fairly well at low velocity. A gradually higher power is required at higher velocity. The best straight-line fit over the complete range of V_N would be about $V_N^{9.5}$.

One might expect jet impingement on the board to be a dipole noise source such that a sixth power curve would fit the data. Figure 10 clearly shows that V_N^6 will not fit the data. The analyses by A. Powell (ref. 9) and O. A. Phillips (ref. 10) showed that jet impingement on a surface need not be a dipole noise generator. Both authors essentially concluded that a large, flat, rigid surface could be a quadrupole noise generator (V_N^8) provided no significant noise is generated by the flow leaving the edges of the surface. These requirements appear to describe the experiment performed in this report.

Consider those points and the fact that the impingement only noise follows V_N^8 and not V_N^6. Let us turn the argument around. The noise data followed V_N^8 not V_N^6; therefore, it is possible to have a flat, rigid surface that is large enough to result in a quadrupole noise source.
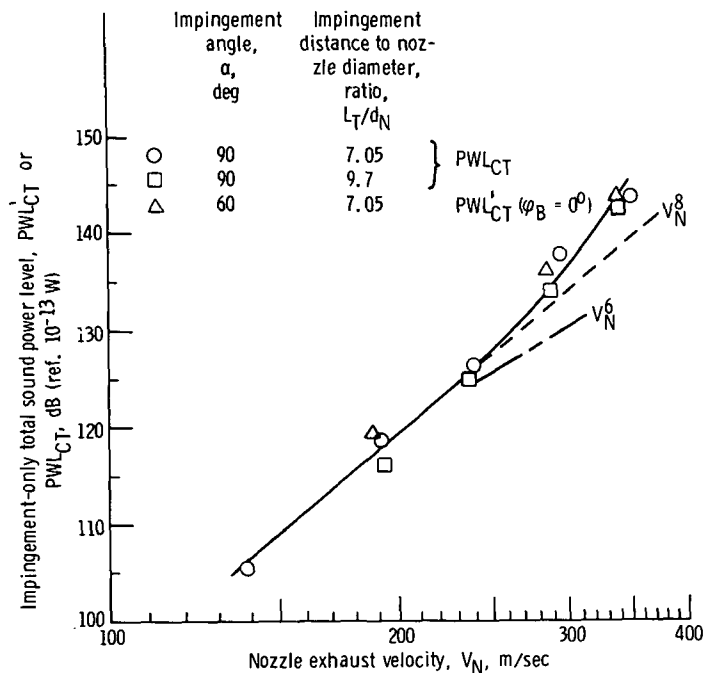

Figure 10. - Variation of impingement-only total sound power level with nozzle exhaust velocity. Nozzle diameter, 5.2 centimeters.

In light of this discussion it would be profitable to consider some results from reference 2. In that paper the impingement noise from the board of this study, and two externally blown flap wings with the nozzle under the wing (a slotted wing and a slotless wing) were compared at the same α and L_T ($\alpha = 60^o$, $L_T = 37$ cm). In both of the wing configurations the total sound power level changed with the sixth power of the jet velocity. But unlike the board, neither of the wing cases have large surfaces, compared with the characteristic wavelength of the noise generated. Also, unlike the board, the exhaust jet from these surfaces was of high velocity. Based on reference 10 it would appear that these are the conditions necessary for the wings to be predominantly dipole noise sources and follow V_N^6. In reference 2 it was shown that the OASPL at different θ follows V_N^6 for the slotted blown flap wing at all values of θ. The slotless wing followed V_N^6 everywhere but below the aircraft ($70^o < \theta < 120^o$), where V_N^8 would be a closer fit. The OASPL for the board follows V_N^8 at all values of θ.

In summary, the impingement-only noise for the large board is essentially proportional to the eighth power of the nozzle exhaust velocity for a given nozzle diameter and impingement distance (or the eighth power of the peak impingement velocity). The large board is therefore predominantly a quadrupole type of noise source.

Effect of Nozzle Diameter

From reference 7 it can be expected that the peak impingement velocity V_{ip} is proportional to the nozzle exhaust velocity V_N and is a function of L_T/d_N. In the previous section it was established that the impingement-only noise for the board was essentially proportional to V_N^8. Therefore, the noise would be proportional to V_{ip}^8 for the 5.2-centimeter-diameter nozzle at a given L_T. In this section the nozzle diameter d_N will be varied for a fixed V_{ip} and α. To keep V_{ip} constant, it is necessary that V_N be held constant, and the impingement distance L_T must also be changed with each change in d_N in order to maintain a constant L_T/d_N. Under these conditions the characteristic impingement diameter d_i would be proportional to d_N. This diameter d_i is discussed in a later section.

Figure 11 is a plot of the impingement-only sound power level spectra PWL_C for the board, for $d_N = 2.7$, 4.1, and 5.2 centimeters, where $\alpha = 90^o$, $V_N = 289$ meters per second, and $L_T/d_N = 9.7$. The spectra are essentially similar in shape, but the noise level increases as d_N^2 and the peak noise frequency varies with $1/d_N$. Figure 12 is a similar plot where $\alpha = 60^o$, $L_T/d_N = 7.05$, and $V_N = 188$ meters per second. The total sound power levels for these two sets of impingement only noise are plotted in figure 13 as a function of nozzle diameter to show the effect of d_N more clearly. A d_N^2 (or d_i^2) curve fits each set of data.
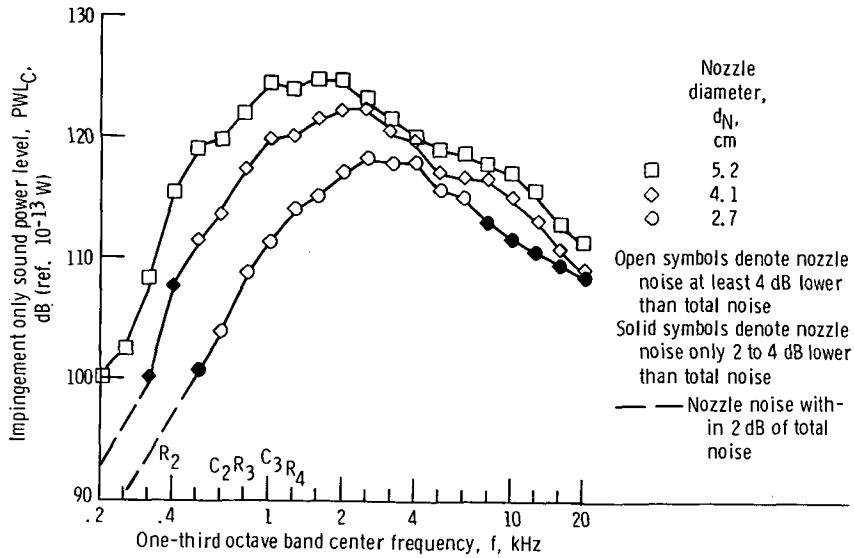
Figure 11. - Variation of impingement-only sound power level spectra with nozzle diameter. Nozzle exhaust velocity, V_N, 289 meters per second; impingement angle, σ, 90^0; impingement distance to diameter ratio, L_T/d_N, 9.7.
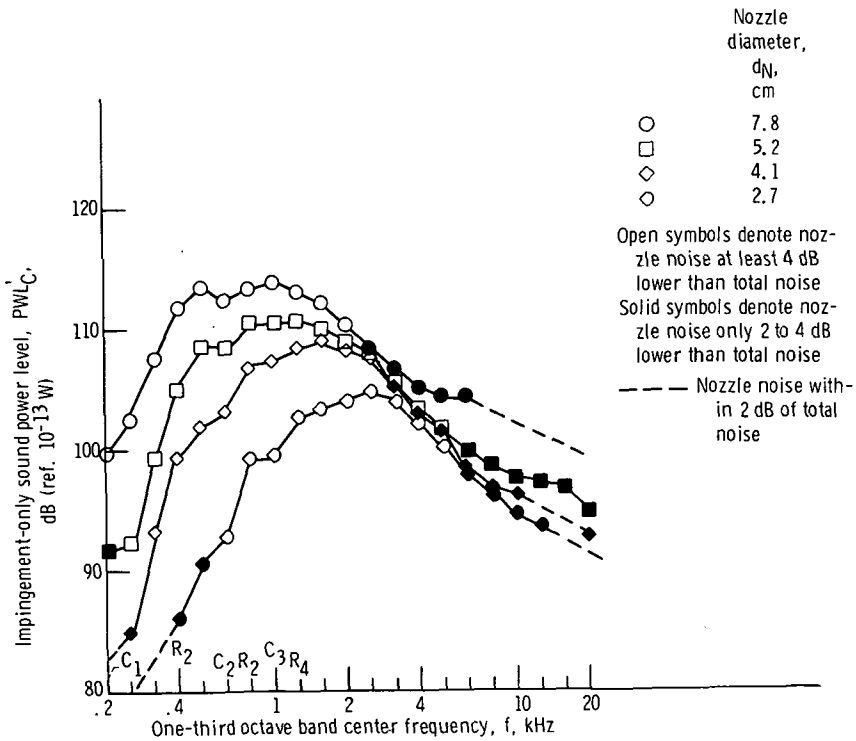

Figure 12. - Variation of impingement-only sound power level (evaluated at $\varphi_B = 0^0$) with nozzle diameter. Nominal nozzle exhaust velocity, V_N, 188 meters per second; impingement angle, σ, 60^0; impingement distance to nozzle diameter ratio, L_T/d_N, 7.05.

17

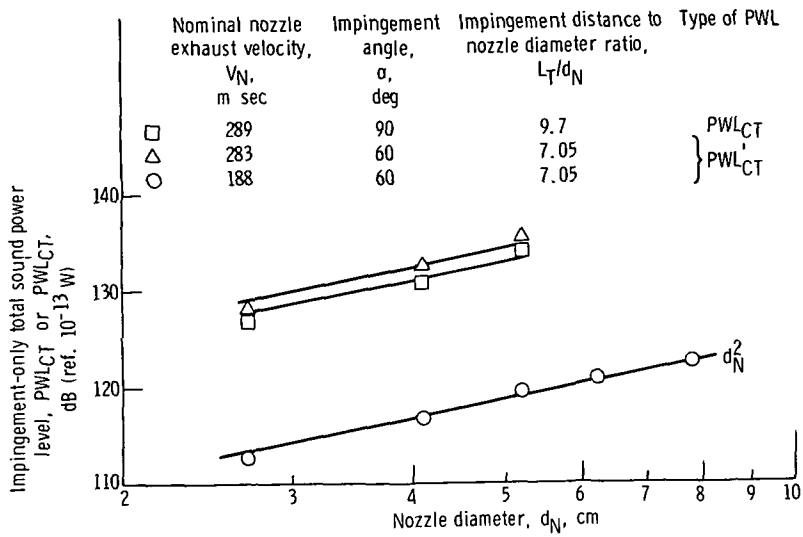|	Nominal nozzle exhaust velocity, V_N, m sec	Impingement angle, α, deg	Impingement distance to nozzle diameter ratio, L_T/d_N	Type of PWL
□	289	90	9.7	$\}$ PWL_{CT}
△	283	60	7.05	$\}$ PWL_{CT}'
○	188	60	7.05	

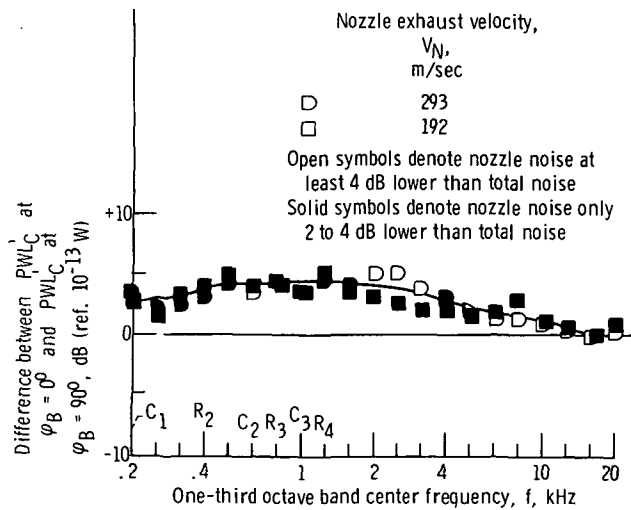Figure 13. - Variation of impingement-only total sound power level with nozzle diameter.

Figure 14. - Change in impingement-only sound power level spectrum when measured and evaluated at maximum noise plane, ($\varphi_B = 0^0$) compared to when at minimum noise plane ($\varphi_B = 90^0$). Impingement angle, α, 60^0; impingement distance to nozzle diameter ratio, L_T/d_N, 7.05.

18

In figure 12 the impingement is not at $\varphi_B = 90^O$; therefore, the noise is not axisymmetric. The impingement-only sound power level spectra plotted in figure 12 are thus only a measure of the power spectra PWL'_C because the noise measurements were taken in one plane ($\varphi_B = 0^O$) and PWL'_C was calculated by assuming that the noise was axisymmetric. To get an idea of the azimuthal variation of PWL'_C with φ_B, the board at $\alpha = 60^O$ was rotated 90° about the nozzle centerline, and the noise was measured again. The PWL'_C was computed the same way again for this minimum noise orientation ($\varphi_B = 90^O$). Figure 14 contains a plot of the difference between the PWL'_C spectra for $\varphi_B = 0^O$ and $\varphi_B = 90^O$ (where $\alpha = 60^O$, $L_T/d_N = 7.05$), and for two velocities. This curve indicates that this difference is independent of V_N (or V_{ip}) and that the $\varphi_B = 0^O$ (maximum noise) orientation is no more than 4 decibels noisier than the $\varphi_B = 90^O$ orientation at $\alpha = 60^O$. Since the peak noise occurs at a frequency where this difference is about 4 decibels, it is estimated that at $\alpha = 60^O$ the azimuthally averaged total power is about 2 decibels less than the maximum noise orientation ($\varphi_B = 0^O$) value PWL'_{TC}. The azimuthal difference can be expected to increase with decreasing impingement angle α.

Effect of Impingement Angle

The effect of the jet impingement angle α on the impingement-only noise is discussed in this section. The loss of axial symmetry in the noise distribution when the jet impingement is not normal ($\alpha < 90^O$) means that extensive noise measurements would be required in several azimuthal planes in order to determine the azimuthally averaged impingement-only sound power level. Instead, the measurements at various α were essentially limited to the maximum noise plane ($\varphi_B = 0^O$). Figure 15 shows the change in PWL'_C, which is evaluated at $\varphi_B = 0^O$, as the impingement angle α decreases at constant V_{ip} and d_i (i.e., constant L_T/d_N, d_N and V_N). The noise level decreased with decreasing α. The center frequency also apparently decreased, but this is discussed further in a later section. Figure 16 shows the variation with α of the measure of the total sound power level PWL'_{CT} which was derived from the spectra plotted in figure 15. Figure 16 shows PWL'_{CT} evaluated at the maximum noise plane ($\varphi_B = 0^O$) and at the minimum noise plane ($\varphi_B = 90^O$). A $\sin^2 \alpha$ curve correlates the maximum noise plane data points well for $\alpha > 15^O$. The $\sin^2 \alpha$ function fails as α approaches zero because the noise could not go to zero. The square symbol at $\alpha = 60^O$ and the data point at $\alpha = 90^O$ describe part of the variation with α in the minimum noise plane ($\varphi_B = 90^O$). The impingement noise could not be measured for $\alpha < 60^O$ because the nozzle-alone noise floor was reached. The impingement-only noise appears to decrease with decreasing α much more rapidly in the $\varphi_B = 90^O$ plane than in the $\varphi_B = 0^O$ plane.
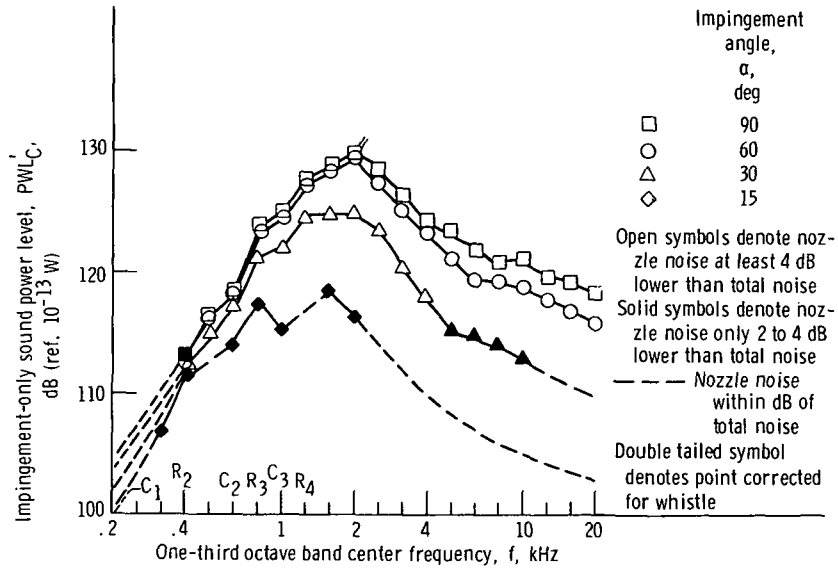
Figure 15. - Variation of impingement-only sound power level spectra evaluated at $\varphi_B = 0^o$, with impingement angle. Nominal nozzle velocity, V_N, 286 meters per second; impingement distance to nozzle diameter ratio, L_T/d_N, 7.05.

Figure 16. - Variation of impingement-only total sound power level, evaluated at φ_B, with impingement angle. Nominal nozzle velocity, V_N, 286 meters per second; impingement distance to nozzle diameter ratio, L_T/d_N, 7.05.
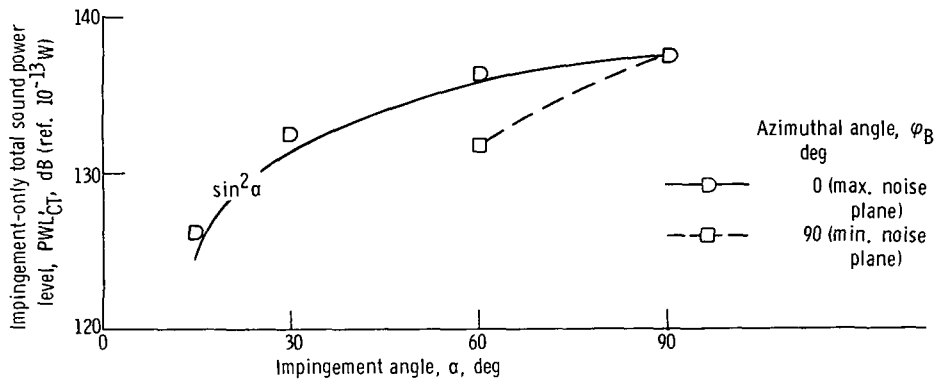
Effect of Nozzle Shape

The effects of nozzle exhaust velocity and nozzle diameter on the impingement-only noise have been established previously. But the shape of the nozzle should also affect the noise because it will affect the impingement velocity. To determine this effect air jets from orifice type nozzles of different shapes, but the same total hole area, were directed at the board. The nozzle exhaust velocity was nearly the same ($V_N = 290$ m/sec), and the board was at $L_T = 15.2$ centimeters and $\alpha = 90^o$. The shapes were a single hole of diameter 4.15 centimeters, four holes (diam 2.07 cm), four holes of the

same size spaced further apart, a slot (1.04×12.7 cm), and 16 holes (1.03 diam). Velocity profiles were measured without the board in place at the impingement distance (L_T = 15.2 cm) for these nozzles. These profiles are shown in figure 17. The impingement velocity profiles are quite different. The jets for the four-hole orifices hit the board as four separate jets; the jets of the 16-hole orifice have formed a well mixed low-velocity stream. The jet from the slot orifice is similar to that of a single hole but of lower velocity at the point of impingement.
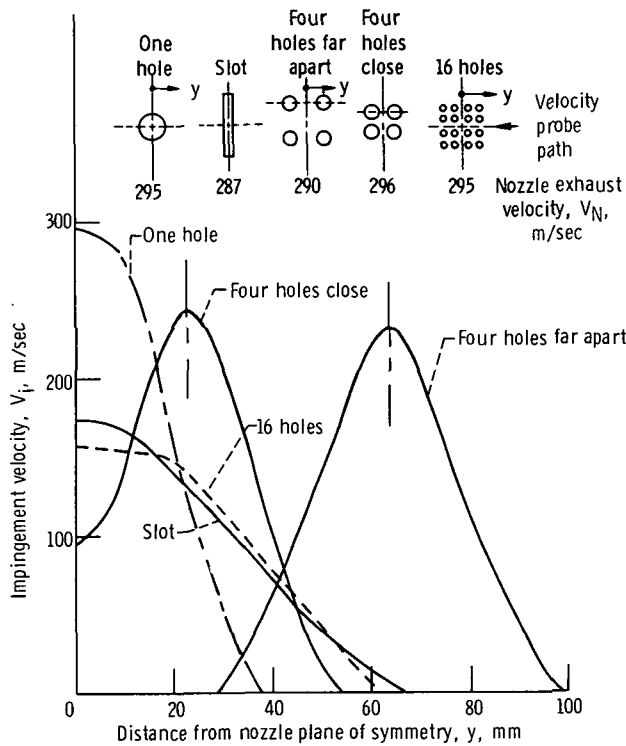

Figure 17. – Measured impingement velocity profiles for five nozzle orifice shapes. Impingement distance, L_T, 15.2 centimeters; nozzle total hole area, 13.2 centimeters.

The impingement-only sound power level spectra for four of these cases is plotted in figure 18. The single hole spectrum was not included because a strong feedback screech noise occurred. The low-frequency low-level impingement noise of the 16-hole and slot orifices go with their low-impingement velocity; the high frequency higher level noise goes with the high impingement velocity of the four hole orifices.

These noise and impingement velocity data will be correlated in a later section.
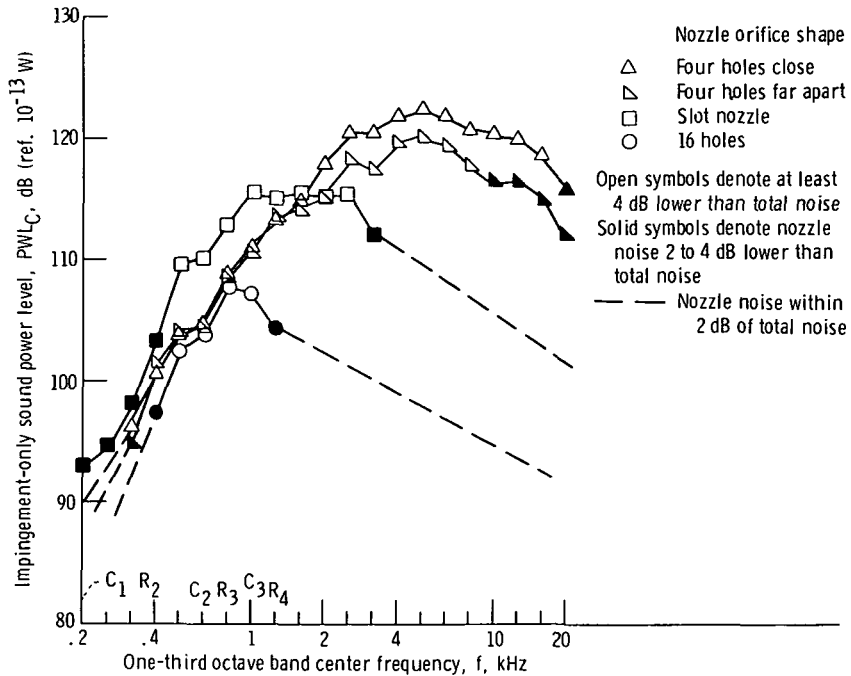
Figure 18. – Variation of impingement-only sound power level spectra with nozzle orifice shape. Nominal nozzle exhaust velocity, V_N, 292 meters per second; nozzle total hole area, 13.2 square centimeters; impingement angle, α, 90°; impingement distance, L_T, 15.2 centimeters.

Effect of Impingement Distance

The distance between the 5.2-centimeter single hole nozzle and the board L_T was varied from $L_T/d_N = 1.9$ to 14.5 diameters at fixed α and V_N ($\alpha = 90^o$ and $V_N = 295$ m/sec). Not only will the impingement velocity change, but feedback whistle and screech, largely avoided in the previous data, may occur. In addition, the noise from the nozzle alone, which is generated within about 10 diameters, should be affected by bringing the board in close to the nozzle. This last expectation is nicely illustrated in figure 19, where the sound power level spectra PWL for the nozzle-alone noise and total noise (impingement + nozzle) at various L_T/d_N are plotted. Compare the nozzle-alone noise to the total noise at low frequency. When L_T/d_N is less than about 7 diameters, a significant part of the low-velocity nozzle-alone noise (low-frequency noise) is apparently being cut off by the board. Feedback noise occurred (tailed symbols) at $L_T/d_N = 4.7$ and 7.05 diameters and was approximately corrected to the double-tailed symbols. The impingement only sound power level spectra PWL_C were determined. Wherever the total noise is less than the nozzle-alone noise, the impingement-only spectra were extrapolated. Figure 20 contains the impingement-only sound power level spectra. It shows that the peak impingement-only noise is about the same for L_T/d_N
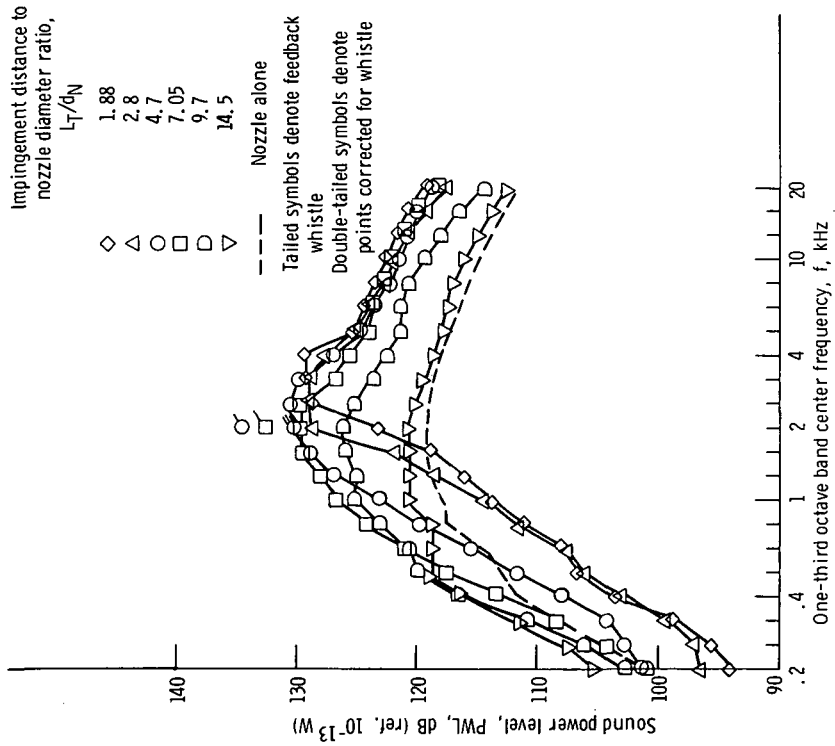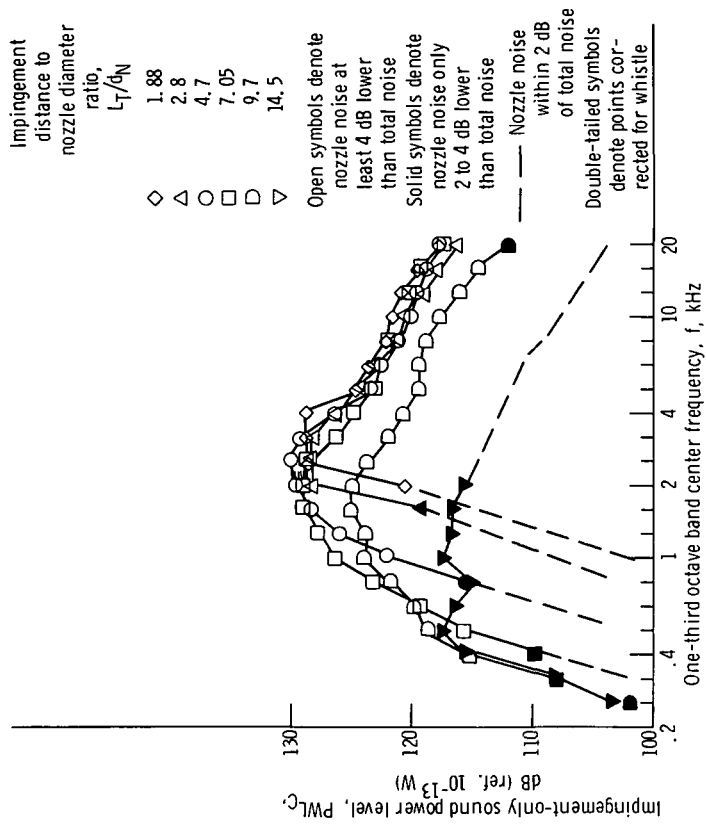
Figure 20. - Variation of impingement-only sound power level spectra with impingement distance. Nominal nozzle exhaust velocity, V_N, 293 meters per second; impingement angle, α, $90°$; nozzle diameter, d_N, 5. 2 centimeters.

Impingement distance to nozzle diameter ratio, L_T/d_N

◇ 1.88
◁ 2.8
○ 4.7
□ 7.05
⬠ 9.7
▷ 14.5

Open symbols denote nozzle noise at least 4 dB lower than total noise

Solid symbols denote nozzle noise only 2 to 4 dB lower than total noise

— — — Nozzle noise within 2 dB of total noise

Double-tailed symbols denote points corrected for whistle

Figure 19. - Variation of sound power level spectra with impingement distance. Nominal nozzle exhaust velocity, V_N, 293 meters per second; impingement angle, α, $90°$; nozzle diameter, d_N, 5. 2 centimeters.

Impingement distance to nozzle diameter ratio, L_T/d_N

◇ 1.88
◁ 2.8
○ 4.7
□ 7.05
⬠ 9.7
▷ 14.5

— — — Nozzle alone

Tailed symbols denote feedback whistle

Double-tailed symbols denote points corrected for whistle

23

less than about 7. The noise level then drops for increasing L_T/d_N. When the board is close ($L_T/d_N < 5$), the low-frequency part of the spectrum is being cut off. This is partly due to the fact that at small L_T/d_N very little of the impingement velocity profile is at low velocity. Another part of the cause is the cut off of the production of low-frequency nozzle-alone noise by the board. Whatever the cause, the low-frequency part of the impingement-only noise spectrum shown in figure 20 is at best approximate.

Overall Correlation of the Impingement-Only Noise

In this section the total sound power level and spectral distribution of the impingement-only noise are correlated with the velocity profile data at the impingement distance from the board.

Total impingement-only sound power level. - In a previous section the jet from a given nozzle was directed at the board at various exhaust velocities while holding the impingement distance and angle constant. It was observed that the impingement-only total sound power level PWL_{CT} correlated well with the eighth power of either the nozzle exhaust velocity or the peak impingement velocity. In the last two sections the nozzle shape and impingement distance were varied at constant exhaust velocity. These results showed that nozzle velocity was not the correct velocity to correlate impingement noise. Impingement velocity was the better choice. The impingement velocity profiles were measured with no board present. Reference 11 indicated that the best correlations of flow and shear stress along the board were achieved by using the impingement velocity measured in this way. It was also observed that the impingement-only noise level was correlated by the square of the nozzle diameter, when the impingement angle and velocity were held constant. This implies that the impingement-only noise would be correlated by the impingement area or the square of some convenient impingement diameter. In addition, the impingement angle α was varied at constant impingement velocity and area. The total sound power level evaluated at the maximum noise plane ($\varphi_B = 0^O$), PWL'_{CT}, was correlated by $\sin^2\alpha$.

Putting these separate correlations together it is reasonable to assume that the total sound power of the impingement-only noise PWL_{CT} would correlate with $V_{ip}^8 A_i$ when $\alpha = 90^O$. When $\alpha < 90^O$, it should be expected PWL'_{CT} would correlate with an impingement parameter given by $\sin^2\alpha\, V_{ip}^8 A_i$. The impingement area is defined by $A_i = l_s d_i$ for the slot nozzle and $A_i \simeq (\pi/4)d_i^2$ for the other cases. The characteristic impingement diameter or width d_i is arbitrarily taken as the dimension, measured from the impingement velocity profile where the velocity is 80 percent of the peak impingement velocity V_{ip}. The noise at 80 percent of the peak velocity would be down about

8 decibels, based on V_i^8. The integral $\int_A V_i^8 \, dA$ could have been used instead of $V_{ip}^8 A_i$. But for a given impingement distance and nozzle shape $V_{ip}^8 A_i$ only differs from $\int_A V_i^8 \, dA$ by a multiplying constant for all the cases of this report. Therefore, $V_{ip}^8 A_i$ is preferred because it requires only two numbers (V_{ip} and d_i). Impingement velocity profiles were measured for most of the cases in this report. The resulting peak impingement velocities and diameters (V_{ip} and d_i) are listed in table I. The impingement data are in excellent agreement with the correlations described in reference 12. These correlations permit the reader to estimate V_{ip} from V_N, L_T/d_N, etc., for many shapes of single nozzles and multiple hole nozzles.

The impingement-only noise total sound power for all the cases in this report are plotted in figure 21 as a function of $\sin^2 \alpha \, V_{ip}^8 A_i$. The figure shows data for normal im-

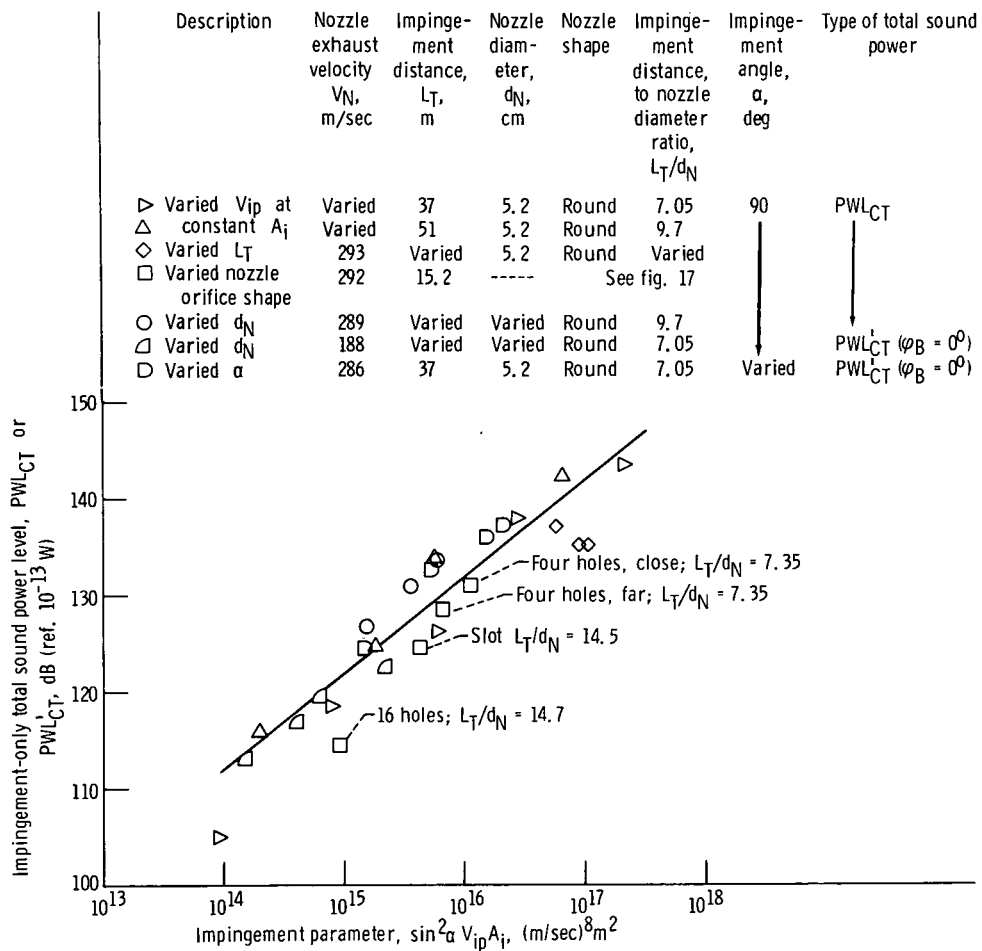|	Description	Nozzle exhaust velocity V_N, m/sec	Impinge-ment distance, L_T, m	Nozzle diam-eter, d_N, cm	Nozzle shape	Impinge-ment distance, to nozzle diameter ratio, L_T/d_N	Impinge-ment angle, α, deg	Type of total sound power
▷	Varied V_{ip} at	Varied	37	5.2	Round	7.05	90	PWL_{CT}
△	constant A_i	Varied	51	5.2	Round	9.7		
◇	Varied L_T	293	Varied	5.2	Round	Varied		
□	Varied nozzle orifice shape	292	15.2	-----	See fig. 17			
○	Varied d_N	289	Varied	Varied	Round	9.7		
◁	Varied d_N	188	Varied	Varied	Round	7.05		$PWL'_{CT} \, (\varphi_B = 0°)$
◻	Varied α	286	37	5.2	Round	7.05	Varied	$PWL'_{CT} \, (\varphi_B = 0°)$

Figure 21. - Correlation of all board impingement only total sound power level data with the peak impingement velocity, V_{ip}, and the impingement area, A_i.

pingement, where $\sin^2 \alpha = 1$ and PWL_{CT} is used because the noise field is axisymmetric, and for the $\alpha < 90^{\circ}$ case where the total power PWL'_{CT} is evaluated at the maximum noise plane ($\varphi_B = 0^{\circ}$). The correlation is good except for the cases where the nozzle was very close to the board and for 16-hole nozzle. In these cases the PWL_C spectral shape is significantly different than for the other cases considered. Comparison of figures 18 and 20 with the other cases shows that the low frequency part of the spectra for the close in board is lower; while the high frequency part of the 16-hole spectra is low. This decrease accounts for their lower total power. A slightly better correlation over the whole range of velocity is achieved if $V_{ip}^{9.5}$ is used instead of V_{ip}^{8}.

Impingement-only noise spectra. - The next task is to correlate the spectral, or frequency, distribution of the impingement only noise. This is accomplished by a normalized correlation where the dimensionless power spectral density of the impingement only noise $DPSD_C$ is plotted as a function of a Strouhal number. From the previous discussion a Strouhal number based on the peak impingement velocity V_{ip} and characteristic impingement diameter d_i would seem to be a good choice. Based on reference 2, $DPSD_C$ is defined (for $\alpha = 90^{\circ}$) as

$$DPSD_C = 10 \log_{10}\left(\frac{V_{ip}}{\Delta f_b d_i}\right) + PWL_C - PWL_{CT}$$

and the impingement Strouhal number is given by

$$S_i = f\frac{d_i}{V_{ip}}$$

The first $DPSD_C$ plot to consider is figure 22, where the spectral data associated with variations of V_N and d_N at $\alpha = 90^{\circ}$ are plotted. No extrapolated PWL_C spectral data are plotted on these Strouhal correlation plots. The continuous-line curves define the bands these data lie within. These bands will be compared with subsequent Strouhal correlation plots. The dashed curves enclose the nozzle-alone noise spectral data reported by reference 4 and this report. The board spectra are sharper than the spectra for the nozzle.

In a previous section it was noted that the impingement-only noise center frequency decreased with decreasing impingement angle α. To better estimate the effect of α, a Strouhal correlation plot is shown in figure 23(a). The correlation is not too good. But if V_{ip}/d_i is multiplied by $\sin^{1/2}\alpha$ then the correlation becomes much better and falls within the band (see fig. 23(b)). To complete the effect of impingement angle, some
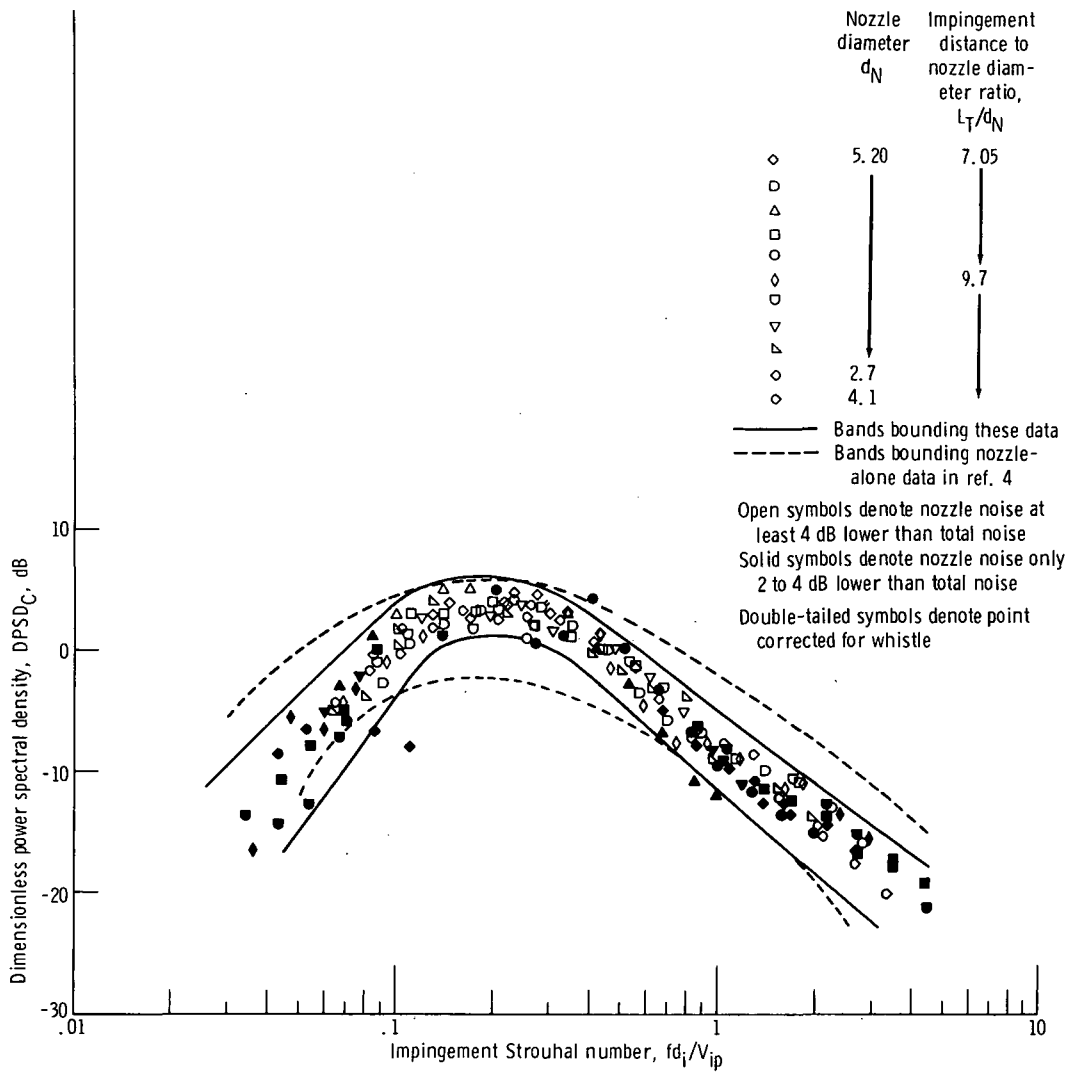
Figure 22. – Strouhal correlation of impingement-only noise data for round nozzles and normal impingement ($\alpha = 90^0$).
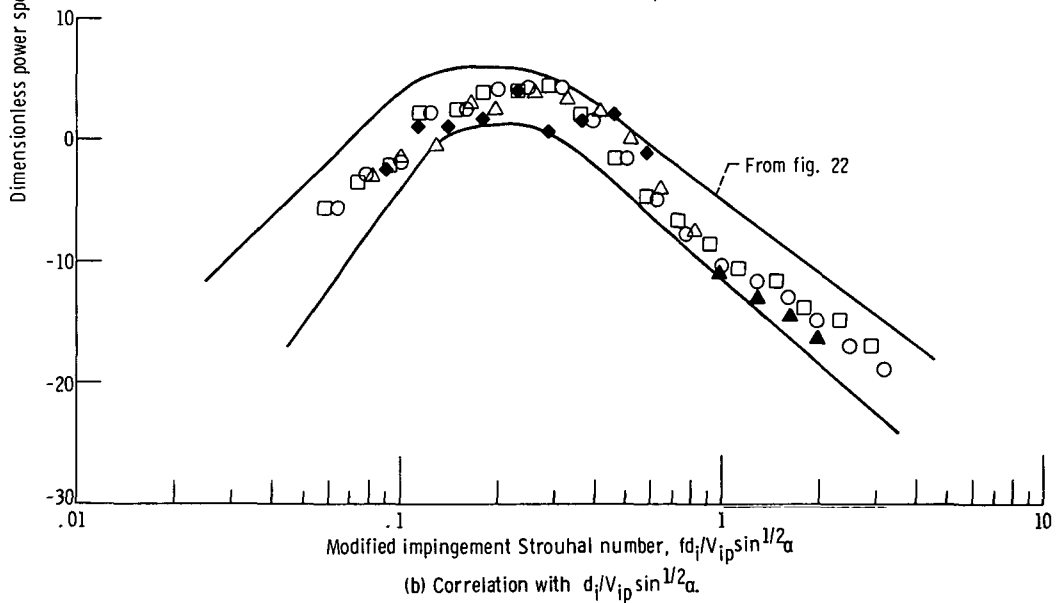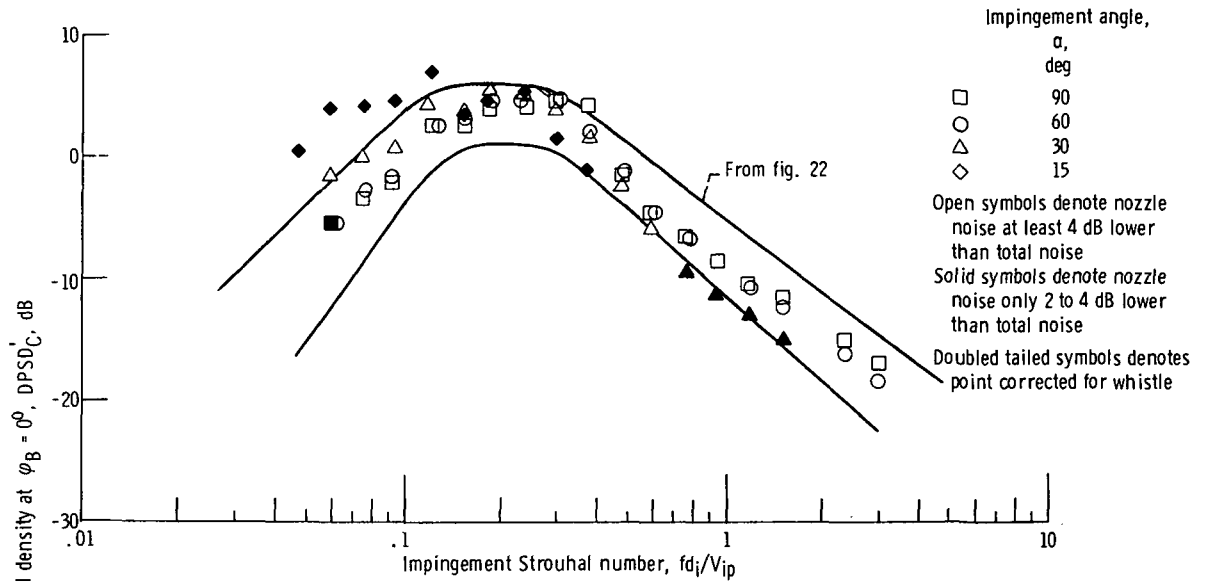
Figure 23. - Effect of impingement angle on Strouhal correlation. Nominal nozzle velocity, V_N, 286 meters per second; impingement distance diameter, L_T/d_N, 7.05; nozzle diameter, 5.2 centimeters.

data taken at $\alpha = 60°$ to show the effect of nozzle diameter are correlated with $d_i/(V_{ip} \sin^{1/2} \alpha)$ in figure 24.

The Strouhal correlation for the cases where the nozzle shape was changed are shown in figure 25. The correlation is good for $S_i > 0.1$; the low-frequency data diverge from the band. Figure 26 contains the Strouhal correlation for the cases where L_T/d_N was varied. Here again, the correlation is good for $S_i > 0.1$ and diverges for the low-frequency data where $L_T/d_N < 5$.
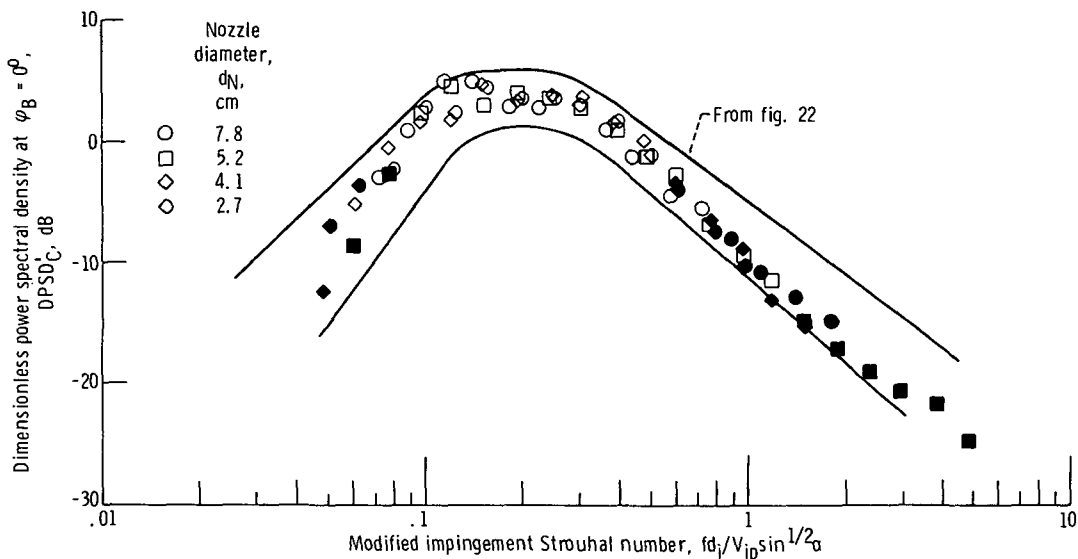

Figure 24. – Effect of nozzle diameter at 60° impingement angle where correlation uses $d_i/V_{ip} \sin^{1/2}\alpha$. Nominal nozzle velocity, V_N, 188 meters per second; impingement distance to nozzle diameter ratio, L_T/d_N, 7.05.
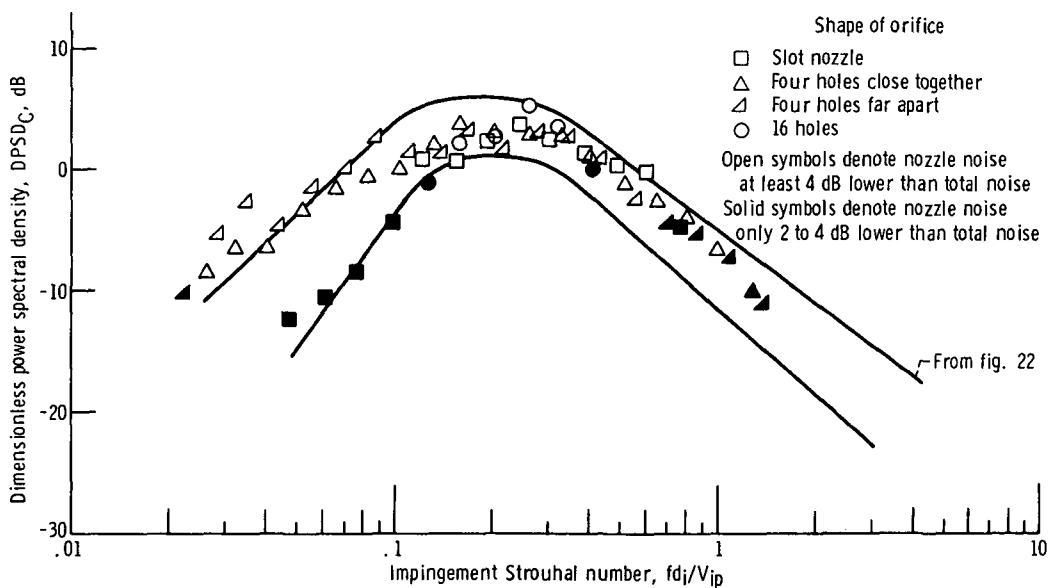

Figure 25. – Effect of nozzle shape on Strouhal correlation. Impingement angle, α, 90°; nozzle orifice area, 13.2 square centimeters, impingement distance, L_T, 15.2 centimeters.
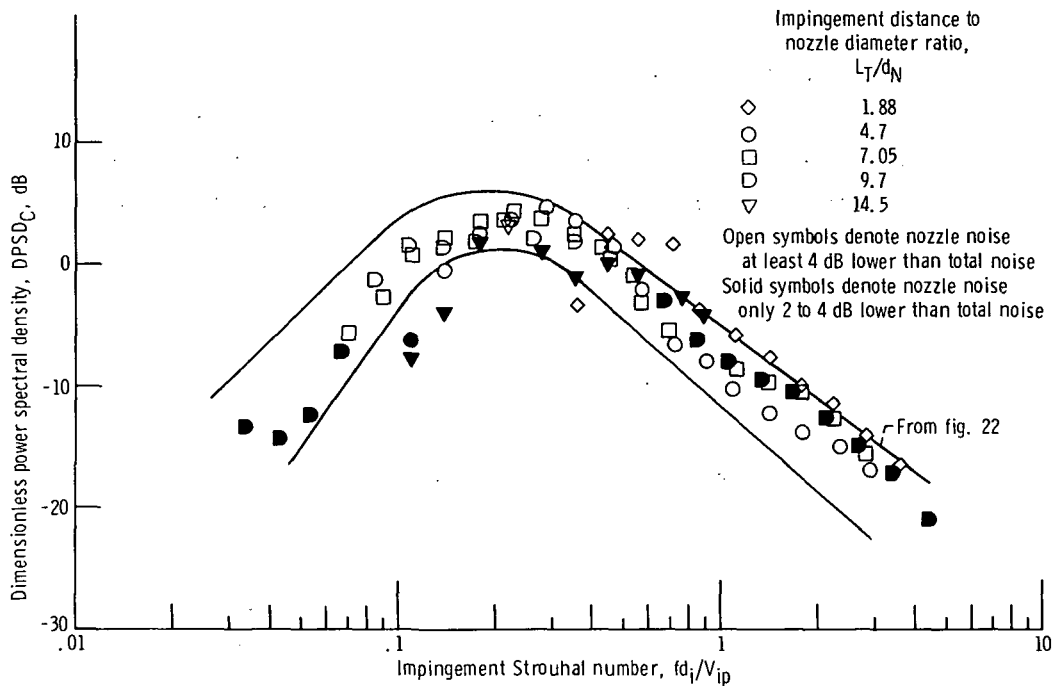
Figure 26. – Effect of impingement distance on Strouhal correlation. Impingement angle, α, 90°; nozzle diameter, d_N, 5.2 centimeters; nominal nozzle exhaust velocity, V_N, 293 meters per second.

SUMMARY OF RESULTS

The noise generated by an air jet impinging on a very large flat plate has the following major characteristics:

1. The shape of the total noise (impingement and nozzle) radiation pattern is essentially independent of nozzle velocity and reaches its maximum near 20° from the board (downstream end).

2. The impingement-only noise (total sound power level) was correlated by the eighth power of the peak impingement velocity and first power of the impingement area. The spectral data were correlated by a Strouhal number based on the peak impingement velocity and a characteristic impingement diameter. When the jet impingement is not normal, the total sound power level is reduced by the square of the sine of the impingement angle, and the Strouhal number is multiplied by the reciprocal of the square root of the sine of the impingement angle.

Lewis Research Center,
   National Aeronautics and Space Administration,
      Cleveland, Ohio, July 6, 1972,
         741-72.

APPENDIX – SYMBOLS

A area normal to nozzle centerline at L_T, m^2

A_i impingement area at L_T, based on d_i, that is normal to the nozzle centerline, m^2

$C_1, C_2, \ldots$ first, second, etc., cancellation frequencies for ground reflections, Hz

d_N nozzle diameter, m

d_i diameter of impingement velocity V_i profile where velocity has dropped to 80 percent of the peak impingement velocity, m

f frequency, Hz

Δf_b width of one-third octave band frequency, Hz

L_T impingement distance; distance along nozzle centerline from nozzle to board, m

ℓ_s length of slot

OASPL   overall sound pressure level, dB

PWL   sound power level at a given f, dB

PWL_C impingement-only noise; result of subtracting PWL for nozzle-alone noise from PWL generated by jet striking board, dB

PWL_T total sound power level, dB

PWL_{CT} total PWL_C, dB

PWL', PWL_T' same as PWL and PWL_T but evaluated at φ_B for nonaxisymmetric noise, dB

PWL_C', PWL_{CT}' same as PWL_C and PWL_{CT} but evaluated at φ_B for nonaxisymmetric noise, dB

$R_1, R_2, \ldots$ first, second, etc., reinforcement frequencies for ground reflections, Hz

SPL   sound pressure level (averaged and corrected for losses), dB

S_i impingement Strouhal number, $f\, d_i / V_{ip}$

V_i impingement velocity; velocity profile measured at impingement distance L_T without presence of board, m/sec

V_{ip} peak impingement velocity, m/sec

V_N nozzle exhaust velocity, m/sec

y   position of velocity probe relative to nozzle cross section axis of symmetry, mm

α impingement angle; smallest angle of nozzle inlet from board, deg

θ angle of microphone from the nozzle inlet (in microphone plane), deg

φ_B azimuthal angle; angle of microphone plane with respect to plane defined by the nozzle centerline and A-A in fig. 2, deg

REFERENCES

1. Dorsch, R. G.; Krejsa, E. A.; and Olsen, W. A.: Blown Flap Noise Research. Paper 71-745, AIAA, June 1971.

2. Olsen, William A.; Dorsch, Robert G.; and Miles, Jeffrey H.: Noise Produced by a Small-Scale, Externally Blown Flap. NASA TN D-6636, 1972.

3. Dorsch, R. G.; Kreim, W. J.; and Olsen, W. A.: Externally-Blown-Flap Noise. Paper 72-129, AIAA, Jan. 1972.

4. Howes, Walton L.: Similarity of Far Noise Fields of Jets. NASA TR R-52, 1960.

5. Wagner, F. R.: The Sound and Flow Field of an Axially Symmetric Free Jet Upon Impact on a Wall. NASA TT F-13942, 1971.

6. Curle, N.: The Influence of Solid Boundaries on Aerodynamic Sound. Proc. Roy. Soc. (London), Ser. A, vol. 231, no. 1187, Sept. 20, 1955, pp. 505-514.

7. Dealy, J. M.: The Confined Circular Jet With Turbulent Source. Symposium on Fully Separated Flows. Arthur G. Hansen, ed., ASME, 1964, pp. 84-91.

8. Simcox, C. D.: Studies of Shock Related Noise Fields Generated by Hot and Cold Choked Jets. Rep. D6-24486, Boeing Co., 1969.

9. Powell, Alan: Aerodynamic Noise and the Plane Boundary. J. Acoust. Soc. Am., vol. 32, no. 8, Aug. 1960, pp. 982-990.

10. Phillips, O. M.: On the Aerodynamic Surface Sound from a Plane Turbulent Boundary Layer. Proc. Roy. Soc. (London), Ser. A, vol. 234, no. 1198, Feb. 21, 1956, pp. 327-335.

11. Donaldson, Coleman DuP.; and Snedeker, Richard S.: A Study of Free Jet Impingement. I. J. Fluid Mech., vol. 45, Jan. 30, 1971, pp. 281-319.

12. von Glahn, U. H.; Groesbeck, D. E.; and Huff, R. G.: Peak Axial-Velocity Decay with Single- and Multi-Element Nozzles. Paper 72-48, AIAA, Jan. 1972.

"The aeronautical and space activities of the United States shall be conducted so as to contribute . . . to the expansion of human knowledge of phenomena in the atmosphere and space. The Administration shall provide for the widest practicable and appropriate dissemination of information concerning its activities and the results thereof."

— NATIONAL AERONAUTICS AND SPACE ACT OF 1958

NASA SCIENTIFIC AND TECHNICAL PUBLICATIONS

TECHNICAL REPORTS: Scientific and technical information considered important, complete, and a lasting contribution to existing knowledge.

TECHNICAL NOTES: Information less broad in scope but nevertheless of importance as a contribution to existing knowledge.

TECHNICAL MEMORANDUMS: Information receiving limited distribution because of preliminary data, security classification, or other reasons.

CONTRACTOR REPORTS: Scientific and technical information generated under a NASA contract or grant and considered an important contribution to existing knowledge.

TECHNICAL TRANSLATIONS: Information published in a foreign language considered to merit NASA distribution in English.

SPECIAL PUBLICATIONS: Information derived from or of value to NASA activities. Publications include conference proceedings, monographs, data compilations, handbooks, sourcebooks, and special bibliographies.

TECHNOLOGY UTILIZATION PUBLICATIONS: Information on technology used by NASA that may be of particular interest in commercial and other non-aerospace applications. Publications include Tech Briefs, Technology Utilization Reports and Technology Surveys.

Details on the availability of these publications may be obtained from:

SCIENTIFIC AND TECHNICAL INFORMATION OFFICE

NATIONAL AERONAUTICS AND SPACE ADMINISTRATION
Washington, D.C. 20546